

12 Competition between Kondo Effect and RKKY Coupling

Stefan Kettemann
Constructor University Bremen
Campus Ring 1, 28759 Bremen

Contents

1	Introduction	2
2	Formation of magnetic moments	4
3	Kondo effect: screening of magnetic moments	6
4	RKKY coupling between magnetic moments	8
5	Spin competition: the Doniach diagram	10
6	Spin competition in presence of a spectral (pseudo) gap	17
6.1	Band insulator, semiconductor	18
6.2	Pseudo-gap semimetal	19
7	Spin competition in the presence of disorder	21
7.1	Distribution of Kondo temperature and RKKY couplings	21
7.2	Anderson localization – local spectral gaps	23
7.3	Multifractality – local pseudo-gaps	25
7.4	Doniach diagram of disordered systems	28
8	Conclusions and open problems	32

1 Introduction

Localized magnetic moments in metals, for example formed by Fe-atoms in gold, interact with the spins of itinerant electrons in the Fermi sea via exchange couplings J . This results in spin dependent electron scattering, in addition to potential scattering from the impurity potential. Depending on magnetic moment density n_M , magnetic impurity spin S , magnitude and sign of exchange couplings J and temperature T , the metal settles for one of a diverse set of quantum phases, each with very different degrees of spin and charge correlations. If the exchange coupling J with impurity spin $S = 1/2$ is antiferromagnetic, all conduction electrons compete to form a singlet with this localized spin, if J is not sufficiently strong to bind and localize one of the electrons completely into a singlet. This competition leads to strongly enhanced magnetic and normal scattering, measurable as enhanced electrical resistivity, as the temperature is lowered towards and below a temperature T_K . This effect was explained by Kondo [1] and is now known as the Kondo effect. The resistance minimum as function of temperature close to the Kondo temperature T_K [2] occurs since above T_K the resistance decays with temperature, as typical for a metal, while it increases at and below T_K due to Kondo enhanced scattering rate. While such magnetic moments are paramagnetic, contributing a Curie magnetic susceptibility $\chi \sim 1/T$ at higher temperature $T > T_K$, at lower temperature their contribution to the magnetic susceptibility saturates to $\chi \sim 1/T_K$. More recently, it was found that mesoscopic metal wires with dilute magnetic impurities show a pronounced peak at T_K in the temperature dependent dephasing rate, which governs quantum corrections to the conductance, the so called weak localization corrections [3–5], allowing high precision studies of the Kondo screening. The Kondo temperature T_K is a functional of the local exchange coupling J and the local density of states ρ , at and in the vicinity of the Fermi energy ε_F . Remarkably, as the temperature is lowered further, a portion of the conduction electrons settle for a joint screening of the magnetic impurity spin and form the so called Kondo singlet, a highly correlated many body state. For the remaining conduction electrons the magnetic impurity spin seemingly disappears. The electrons settle then again to form a Fermi liquid, albeit with enhanced density of states at the Fermi energy, forming a narrow resonance peak of width $k_B T_K$, as sketched in Fig. 1 (upper Right). As a consequence, the spin scattering from the magnetic impurity decays to zero, as the temperature is lowered further. The remaining enhanced potential scattering from the Kondo impurities then contributes to the enhanced low temperature resistance.

When the concentration of magnetic moments in a metallic host is high, and they form a regular lattice, all Kondo impurities can conspire to form a narrow band at the Fermi energy, as sketched in Fig. 1 (lower Right), at sufficiently low temperature, below a critical temperature $T_c < T_K$. Then, the itinerant electrons at the Fermi energy are no longer scattered from the potential of the Kondo impurities but move through the lattice formed by the Kondo impurities as dressed quasiparticles with strongly enhanced mass, accordingly called *heavy fermions*. This transition to a new state of heavy but itinerant fermions is experimentally seen, when the Fermi energy is in that narrow band, in a sudden drop of the resistivity below a critical temperature T_c , where the low temperature coherence sets in, while at higher temperatures still the typical Kondo enhanced

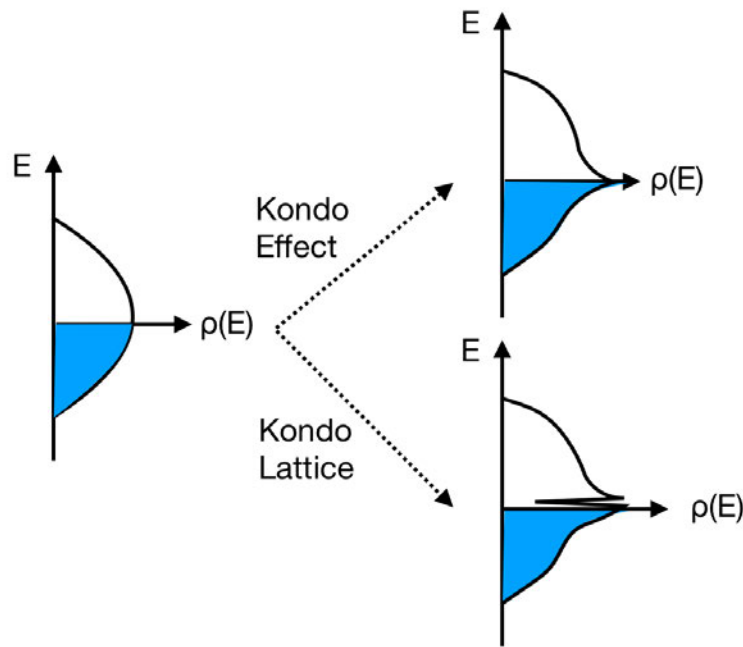


Fig. 1: Left: Sketch of typical density of states $\rho(E)$ of a metal as function of energy E , with states filled up to the Fermi energy ε_F , as colored in blue. Upper Right: For dilute magnetic impurities with spin $S = 1/2$, coupled by an antiferromagnetic exchange coupling to the conduction electron spins, a Kondo resonance of width $k_B T_K$ forms. Lower Right: At sufficiently large impurity density a Kondo lattice forms with a narrow band at the Fermi energy.

resistivity from individual Kondo impurities is observable. This is observed for example in the intermetallic crystal CeCu_6 , where the Ce^{3+} -ions form at high temperature a dense lattice of magnetic moments in the metallic copper host, while at low temperatures a transition to a coherent state of heavy electrons occurs with a sharp drop of resistivity [6–9].

However, localized magnetic moments in metals interact with each other. Their magnetic dipole interaction is finite, but is typically exceeded by far by indirect exchange couplings between them, the so called RKKY couplings, mediated by conduction electrons [10–12]. In metals, RKKY coupling decays slowly, with a power law of distance R between two magnetic moments. The RKKY coupling is a functional of exchange couplings J , local density of states at the Fermi energy at the locations of the magnetic impurities $\rho(\mathbf{r}, E_F)$, and their distance R . Since these couplings tend to quench their spins, it may prevent the Kondo screening by the conduction electrons partially, or even completely, depending on the amplitude of local exchange coupling J , the distance R between them and temperature T .

Thus, there is a competition between Kondo screening and RKKY coupling. Depending on which one wins, the system will find itself in very different quantum states. This competition can be studied systematically by increasing the density of magnetic impurities. Increasing their concentration, decreases their average distance R and thereby the typical RKKY coupling between them increases. In the very dilute limit RKKY couplings can be neglected, and magnetic impurities can be treated as a dilute set of single Kondo spins, as shown in Fig. 2a). Increasing

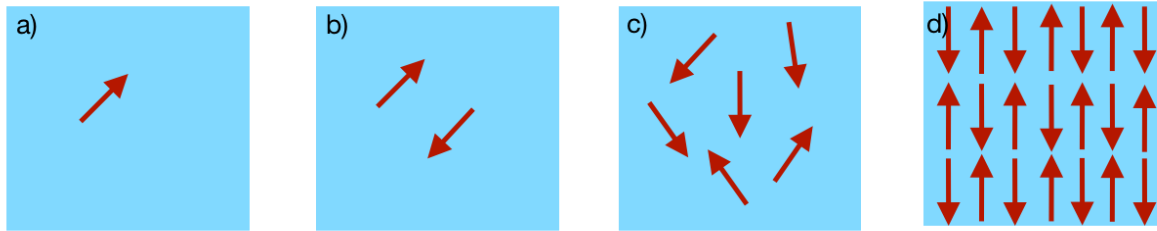


Fig. 2: Kondo impurity spins (red) in a metal host (blue): a) Single Kondo impurity, b) Pair of Kondo impurities, c) Dilute Kondo system, d) Kondo lattice.

their concentration further, randomly placed magnetic impurities may be modeled by a set of pairs of magnetic impurities, formed by those spins which are closest to each other, as shown in Fig. 2b). At higher concentrations larger clusters of spins, shown in Fig. 2c) have to be considered to model their quantum state, and at still higher concentrations a connected random network of them. When the density of magnetic moments is so high that they form a regular lattice, as it occurs in f -band materials, a coherent Kondo lattice can form. The competition between the Kondo effect in this Kondo lattice and the RKKY coupling gives rise to a quantum phase transition between a heavy fermion state and an ordered state, which, when mapped as function of exchange coupling J , is called the Doniach diagram [13, 14].

In these lecture notes we give an introduction to the theory of this rich competition between Kondo screening and RKKY coupling. In section 2 we review the formation of magnetic moments as modeled by the Anderson model. In section 3 we review the theory of the Kondo effect for a single magnetic impurity in a metal host. In section 4 we derive the RKKY coupling between magnetic impurities in a metal host. In section 5 we review the Doniach diagram, and give an introduction to a self consistent renormalization group theory which takes into account both Kondo effect and RKKY coupling between magnetic impurities, and explain the results obtained thereby. In section 6 we review the effect of gaps and pseudo-gaps on both Kondo effect and RKKY couplings, and accordingly on their competition. Especially for dilute concentration of magnetic moments, the disorder effects from randomly distributed impurities result in a distribution of both Kondo temperatures and RKKY couplings. Then, their competition becomes an even more complex problem, as reviewed in section 7. Moreover, disorder induced Anderson localization transitions may occur, which effect both Kondo effect and RKKY coupling severely, and changes their competition, as we review in that section, as well. We conclude with an outlook and list the, in our view, most pressing and interesting open problems.

2 Formation of magnetic moments

The first microscopic model for the formation of magnetic moments in metals was formulated by P.W. Anderson [15]. He showed that local moments can form from localized d - or f -levels which are weakly coupled by hybridization to the conduction electrons, when the repulsive Coulomb interaction $U > 0$ between two electrons on these localized levels is sufficiently

large. He found furthermore, quite surprisingly, that the resulting local moments develop an antiferromagnetic coupling with the spins of the surrounding electron liquid. The formation of magnetic moments is described by the Anderson model, where a d - or f -level is weakly coupled to conduction band electrons, as modelled by the Hamiltonian [15]

$$H = \sum_{n,\sigma} E_{n\sigma} \hat{n}_{n\sigma} + \sum_{\sigma} \varepsilon_{d\sigma} \hat{n}_{d\sigma} + U \hat{n}_{d+} \hat{n}_{d-} + \sum_{n,\sigma} (t_{nd} c_{n\sigma}^{\dagger} d_{\sigma} + t_{dn} d_{\sigma}^{\dagger} c_{n\sigma}), \quad (1)$$

where electrons in a conduction band state $|n\rangle$ with eigenenergy $E_{n\sigma}$ are annihilated and created by fermion operators $c_{n\sigma}$, $c_{n\sigma}^{\dagger}$ with spin index $\sigma = \pm$. The corresponding density operator is $\hat{n}_{n\sigma} = c_{n\sigma}^{\dagger} c_{n\sigma}$. In the following, we assume spin degeneracy of the conduction band states $E_{n\sigma} = E_n$. The annihilation and creation operators of electrons in the d -level are d_{σ} , d_{σ}^{\dagger} with density operator $\hat{n}_{d\sigma} = d_{\sigma}^{\dagger} d_{\sigma}$. The d -level can either be in a magnetic state, when it is occupied by a single electron with energy $\varepsilon_{d\sigma}$, which can be in one of two spin states $\sigma = \pm$. We assume that these two states form a Kramers doublet, with energy ε_d , degenerate in the spin σ . Furthermore, it can be in a nonmagnetic state when unoccupied or when doubly occupied, with vanishing total spin and total energy $2\varepsilon_d + U$. In order that the ground state is magnetic, the energy of the singly occupied states must be lower than the energy of the unoccupied state, as well as the one of the doubly occupied state, requiring $\varepsilon_d < 0$ and $\varepsilon_d + U > 0$. Thus, the repulsion must be stronger than the bound state energy of a single electron, $U > -\varepsilon_d$. At finite temperature T , the d -level remains magnetic as long as T is lower than the energy cost for such valence fluctuations, $T < \min(\varepsilon_d + U, -\varepsilon_d)$. However, the hybridization between the d -level and the conduction band state $|n\rangle$, as given by the matrix elements $t_{dn} = t_{nd}^*$, may change this ground state. To study its effect on the magnetic states, one can project nonmagnetic higher energy states, where the d -level is doubly occupied or unoccupied, out of the Hilbert space of the d -level. This was done by Schrieffer and Wolff [16], who thereby showed that the spin on the d -level is coupled by an antiferromagnetic exchange interaction J with the spins of the conduction electrons. Performing this, so called Schrieffer-Wolff transformation one obtains the Kondo Hamiltonian in its most general form

$$H_K = \sum_{n,\sigma} E_n \hat{n}_{n\sigma} + \sum_{n,n'} J_{nn'} \left(S^+ c_{n+}^{\dagger} c_{n'-} + S^- c_{n-}^{\dagger} c_{n'+} + S_z (c_{n+}^{\dagger} c_{n'+} - c_{n-}^{\dagger} c_{n'-}) \right), \quad (2)$$

where \mathbf{S} is the spin vector operator of the localized moment, written here in terms of the ladder operators $S^{\pm} = S_x \pm iS_y$ and its z -component S_z . The matrix elements of the exchange coupling in the basis of the conduction electron eigenstates $|n\rangle$ are found to be given by

$$J_{nn'} = t_{nd} t_{dn'} \left(\frac{1}{U + \varepsilon_d - E_{n'}} + \frac{1}{-\varepsilon_d + E_n} \right). \quad (3)$$

The hopping matrix element connecting the localized d -state $\phi_d(\mathbf{r})$ to the conduction band state $\psi_n(\mathbf{r})$ is related to the atomic potential \hat{V} by the hybridization integral

$$t_{dn} = \langle d | \hat{V} | n \rangle = \int d^d r \phi_d^*(\mathbf{r}) V(\mathbf{r}) \psi_n(\mathbf{r}). \quad (4)$$

For an impurity state strongly localized on a length scale a_0 at position \mathbf{r} in a d -dimensional sample, one can simplify that expression with the hybridization parameter t to

$$t_{dn} \approx t a_0^d \phi_d^*(\mathbf{r}) \psi_n(\mathbf{r}). \quad (5)$$

Assuming that both nonmagnetic states have the same energy $U/2$, one arrives at the symmetric Kondo model. In this approximation, the Kondo Hamiltonian can be written with the superexchange term in the form of a Heisenberg Hamiltonian [1, 8],

$$H_K^0 = \sum_{n,\sigma} E_n \hat{n}_{n\sigma} + J \vec{\mathbf{S}} \vec{\mathbf{s}}(\mathbf{r}), \quad (6)$$

where $J = 4t^2/U > 0$. Thus, the superexchange interaction is indeed antiferromagnetic. The matrix elements of the conduction band spin density vector operator $\vec{\mathbf{s}}(\mathbf{r})$ at the site of the d -level, \mathbf{r} are given by

$$\vec{\mathbf{s}}_{\alpha\beta}(\mathbf{r}) = \sum_{n,n'} \psi_{n'}^*(\mathbf{r}) \psi_n(\mathbf{r}) c_{n\alpha}^\dagger \vec{\sigma}_{\alpha\beta} c_{n'\beta}, \quad (7)$$

where $\vec{\sigma}$ is the vector of Pauli matrices $\vec{\sigma} = (\sigma_x, \sigma_y, \sigma_z)$. Here, we used $a_0^d |\phi_d(\mathbf{r})|^2 = 1$, since the intensity $|\phi_d(\mathbf{r})|^2$ in the d -level is localized in the volume a_0^d .

3 Kondo effect: screening of magnetic moments

When the bare antiferromagnetic exchange interaction J is too weak to bind a single conduction electron into a singlet state, all conduction electrons in the vicinity of the Fermi energy become excited by scattering from the magnetic impurity spin. Integrating out all these excitations, of conduction electrons to energy levels E_m above the Fermi energy and of hole excitations below the Fermi energy, one finds that the exchange interaction J becomes thereby enhanced. Performing perturbation theory to second order in J , there are two processes to be considered: (i) The scattering due to the exchange coupling J of an electron from initial state $|n\rangle$ to a state $|l\rangle$ at the Fermi energy via an intermediate state $|m\rangle$, which can be of either spin. This process is proportional to the probability that state $|m\rangle$ is not occupied, $1 - f(E_m)$, where $f(E)$ is the Fermi distribution function. (ii) The reverse process, in which a hole is scattered from the state $|l\rangle$ to the state $|n\rangle$ via the occupied state $|m\rangle$ which is accordingly proportional to the occupation factor $f(E_m)$. Thereby, one finds that the Kondo exchange Hamiltonian acquires an additional term so that the total exchange coupling becomes

$$\tilde{J}_{nl} = J_{nl} \left[1 + \frac{J}{2N} \sum_{m,\sigma} \frac{L^d |\psi_m(\mathbf{r})|^2}{E_m - E_F} \tanh\left(\frac{E_m - E_F}{2T}\right) \right]. \quad (8)$$

For positive exchange coupling, $J > 0$, the correction term is positive as well. Moreover, this perturbation theory diverges as the temperature is lowered. Defining the Kondo temperature as the temperature where perturbation theory breaks down since the second-order correction to the

exchange coupling becomes equal to the bare coupling, we find in this 1-loop approximation, that the Kondo temperature at site \mathbf{r} of a spin- $1/2$ -impurity is determined by the equation [17, 18]

$$1 = \frac{J}{2N} \sum_{m,\sigma} \frac{L^d |\psi_m(\mathbf{r})|^2}{E_m - E_F} \tanh\left(\frac{E_m - E_F}{2T_K(\mathbf{r})}\right), \quad (9)$$

with N the total number of energy levels, including spin degeneracy, in a finite sample of linear size L and dimension d . $|\psi_m(\mathbf{r})|^2$ is the probability density of the eigenstate at site \mathbf{r} .

An equivalent expression can be derived from a renormalization group analysis. Integrating successively high energy excited states at energy scale Λ above and below the Fermi energy yields the renormalized coupling $\tilde{J}(\Lambda)$, governed by the RG flow equation [19, 20]. For a magnetic moment at site \mathbf{r} with exchange coupling J and local density of states at energy ε , $\rho(\mathbf{r}, \varepsilon)$, the renormalization of the effective coupling $\tilde{J}(\Lambda)$ at energy scale Λ , above and below the Fermi energy, is found in 1-loop approximation to be given by

$$\frac{d\tilde{J}}{d \ln \Lambda} = -\tilde{J}^2 \frac{V_a}{2} (\rho(\mathbf{r}, \varepsilon_F + \Lambda) + \rho(\mathbf{r}, \varepsilon_F - \Lambda)), \quad (10)$$

where $V_a = L^d/N$ is the atomic volume, which is often set equal to one, we will keep it for clarity. The solution of Eq. (10) diverges for small energy scales $\Lambda \rightarrow 0$. Defining the Kondo temperature by the scale $\Lambda_K = k_B T_K$ at which the correction to the renormalized coupling is equal to the bare coupling, we recover Eq. (9), when approximating $\tanh(x) \approx \text{sign}(x)$ for $|x| > 1$, and 0 otherwise, noting that the local density of states, the number of states per energy and volume, can be written in terms of the eigenstates of the conduction electrons as

$$\rho(\mathbf{r}, \varepsilon) = \sum_{n,\sigma} |\psi_n(\mathbf{r})|^2 \delta(\varepsilon - E_n). \quad (11)$$

In terms of the local density of states, we can thus rewrite Eq. (9) as

$$1 = \frac{V_a}{2} J \int_0^D dE \frac{\rho(E, \mathbf{r})}{E - E_F} \tanh\left(\frac{E - E_F}{2T_K(\mathbf{r})}\right). \quad (12)$$

Since perturbation theory breaks down at temperatures of the order of T_K , a nonperturbative treatment is needed to be able to derive lower temperature properties. This is possible with the Wilson numerical renormalization group method [21, 22] and analytically with the exact Bethe-Ansatz method [23, 24]. Both methods show that the temperature T - and magnetic field H -dependence of the free energy, and thus all thermodynamic observables, as well as transport properties like the resistivity, scale with the Kondo temperature, depending only on the ratios T/T_K and H/T_K . Thus, thermodynamic observables like the magnetic susceptibility are for single Kondo impurities proportional to known universal scaling functions of T/T_K and H/T_K , and it only remains to find the Kondo temperature for specific magnetic impurities in a metal. The low temperature phase can thus be described by a state where the magnetic impurity spins are screened by Kondo clouds formed by the conduction electrons whose effective mass is thereby enhanced, but still forming a Fermi liquid [25].

Therefore, let us first proceed to review the calculation of the Kondo temperature T_K . For a clean metal the eigenstates are plane waves with uniform density $|\psi_n(\mathbf{r})|^2 = 1/L^d$, independent of position \mathbf{r} . For a smooth density of states $\rho(\varepsilon_F) = \rho_0$, we denote the number of states per energy and spin as $N_0 = V_a \rho_0/2$, with $V_a = L^d/N$. Then, Eq. (12) simplifies to

$$1 = J \int_0^D dE \frac{N_0}{E - E_F} \tanh\left(\frac{E - E_F}{2T_K}\right). \quad (13)$$

Noting that $\tanh(x) \rightarrow \text{sign}(x)$ for $|x| \gg 1$, and assuming that the Fermi energy is in the middle of the band $E_F = D/2$, we find $1 \approx J 2N_0 \ln(D/T_K)$, yielding the Kondo temperature

$$T_K^0 = cD e^{-1/2N_0J}, \quad (14)$$

where $c = 0.57$ is found by a more accurate integration of the tanh-function. Higher order corrections in J lead only to pre-exponential corrections which depend weakly on J . Thus, the 1-loop result T_K^0 yields already the dominant dependence on the exchange coupling J .

The Kondo effect can also occur in semimetals, semiconductors and even insulators, where the density of states at the Fermi energy is vanishing, when the exchange coupling exceeds a critical value J_c . At first sight, Eq. (14) seems to imply, that the Kondo temperature is vanishing when $\rho(\varepsilon_F) = 0$. However, then the assumption of smooth density of states is no longer valid and we need to start rather from the general self consistency equation, Eq. (9). In section 6 we will therefore consider and review the derivation of the Kondo temperature and J_c for two generic cases: a) when the Fermi level is in a pseudo-gap and b) when it is in a hard gap.

In a real material there are spatial variations of local density of states $\rho(\mathbf{r})$ and exchange coupling J due to inhomogeneities and disorder, both from nonmagnetic and magnetic impurities. According to Eq. (9) this results in Kondo temperatures which vary with spatial position, $T_K(\mathbf{r})$, since the intensity $|\psi_n(\mathbf{r})|^2$ may vary spatially. Moreover the intensity of each state $|n\rangle$ at different energy E_n at the site of a magnetic moment may be different, making it a complex problem to evaluate the sum over all eigenstates. In fact, already in a weakly disordered metal one finds that the Kondo temperature is distributed with a finite width [26–28]. In section 7 we will therefore consider and review the Kondo effect in disordered systems in more detail.

4 RKKY coupling between magnetic moments

A magnetic impurity never comes alone. Thus, we need to consider what happens when more than one magnetic impurity is in the metal. Naturally, the Anderson impurity model Eq. (1) can be extended to any number M of localized level sites, summing over their M positions \mathbf{r}_j ,

$$H = \sum_{n,\sigma} E_{n\sigma} \hat{n}_{n\sigma} + \sum_{j,\sigma} \varepsilon_{d_j\sigma} \hat{n}_{d_j\sigma} + \sum_j U_j \hat{n}_{d_j+} \hat{n}_{d_j-} + \sum_{n,j,\sigma} \left(t_{nd_j} c_{n\sigma}^\dagger d_{j\sigma} + t_{d_jn} d_{j\sigma}^\dagger c_{n\sigma} \right), \quad (15)$$

where the energy of localized levels $\varepsilon_{d_j\sigma}$, onsite interaction U_j , and hopping elements t_{d_jn} may depend on the positions \mathbf{r}_j , where $j = 1, \dots, M$. Nothing prevents us, to perform again a

Schrieffer-Wolff transformation to the Kondo Hamiltonian in the basis of the singly occupied states of the M magnetic moments, which yields

$$H_K = \sum_{n,\sigma} E_n \hat{n}_{n\sigma} + \sum_{j,n,n'} J_{j,nn'} \left(S_j^\dagger c_{n+}^\dagger c_{n'-} + S_j^- c_{n-}^\dagger c_{n'+} + S_{jz} (c_{n+}^\dagger c_{n'+} - c_{n-}^\dagger c_{n'-}) \right), \quad (16)$$

where \mathbf{S}_j is now the spin vector operator of the localized moment at position \mathbf{r}_j . Accordingly, the matrix elements of the exchange coupling depend on the positions \mathbf{r}_j as

$$J_{j;nn'} = t_{nd_j} t_{d_j n'} \left(\frac{1}{U_j + \varepsilon_{d_j} - E_{n'}} + \frac{1}{-\varepsilon_{d_j} + E_n} \right). \quad (17)$$

For the symmetric Kondo model, we then get,

$$H_K = \sum_{n,\sigma} E_n \hat{n}_{n\sigma} + \sum_j J_j \vec{\mathbf{S}}_j \vec{\mathbf{s}}(\mathbf{r}_j) = H_0 + H_J, \quad (18)$$

with $J_j = 4t_j^2/U_j > 0$. To derive the RKKY-coupling at finite temperature T , let us consider the thermodynamic potential Ω for the Kondo model Eq. (16). The correction $\Delta\Omega$ due to the exchange interaction between magnetic moments and the Fermi sea is given by

$$\Delta\Omega = -T \ln \langle S \rangle = -T \ln \left(\text{Tr}(S \cdot e^{-H_0/T}) / Z_0 \right), \quad (19)$$

where Z_0 is the grand canonical partition function of the Fermi sea, and S the correction factor due to the exchange interaction term in the Hamiltonian, H_J , $S = \exp \left(-\int_0^{1/T} H_J(\tau) d\tau \right)$. Performing perturbation theory in J to second order we obtain

$$\Delta\Omega = -\frac{1}{2} T \sum_{i,j;\alpha\beta\gamma\delta} J_i J_j \int_0^{1/T} \int_0^{1/T} d\tau_1 d\tau_2 \left\langle \vec{\mathbf{S}}_i \vec{\sigma}_{\alpha\beta} \vec{\mathbf{S}}_j \vec{\sigma}_{\gamma\delta} T_\tau (c_{i\alpha}^\dagger(\tau_1) c_{i\beta}(\tau_1) c_{j\gamma}^\dagger(\tau_2) c_{j\delta}(\tau_2)) \right\rangle. \quad (20)$$

where $\langle \dots \rangle = \text{Tr}(\dots \exp(-H_0/T)) / Z_0$. Here, we assumed that the conduction electron spins are not polarized, $\langle \vec{\mathbf{s}}(\mathbf{r}) \rangle = 0$. Terms proportional to $\vec{\mathbf{S}}_i^2$ and $\vec{\mathbf{S}}_j^2$ yield only corrections to the local energy, not to the nonlocal interaction J_{RKKY} . With Wick's theorem we can present the correlator in Eq. (20) in the form $-\mathcal{G}_{\beta\gamma}(i, j; \tau_1 - \tau_2) \mathcal{G}_{\delta\alpha}(j, i; \tau_2 - \tau_1)$, where

$$\mathcal{G}_{\beta\gamma}(i, j, \tau_1 - \tau_2) = - \left\langle T_\tau (c_{i\beta}(\tau_1) c_{j\gamma}^\dagger(\tau_2)) \right\rangle \quad (21)$$

is the Matsubara Green function [29]. Since we perform perturbation theory in J to 2nd order only, and as long as there are no other spin dependent couplings in the Hamiltonian, the propagator $\mathcal{G}_{\beta\gamma}$ is proportional to $\delta_{\beta\gamma}$ which allows us to perform the summation over spin indices in Eq. (20) explicitly to get $\sum_{\alpha\beta} \mathbf{S}_i \vec{\sigma}_{\alpha\beta} \mathbf{S}_j \vec{\sigma}_{\beta\alpha} = \mathbf{S}_i \cdot \mathbf{S}_j$. Thus, we find in second order perturbation theory in J that there is an indirect exchange coupling term in the Hamiltonian, the RKKY coupling between the magnetic impurity spin operators $\vec{\mathbf{S}}_i, \vec{\mathbf{S}}_j$, given by

$$H_{\text{RKKY}} = \sum_{i,j} J_i J_j \chi_{ij} \vec{\mathbf{S}}_i \vec{\mathbf{S}}_j, \quad (22)$$

with the non local, temperature dependent susceptibility matrix

$$\chi_{ij} = -\frac{1}{2} \int_0^{1/T} \mathcal{G}(i, j; \tau) \mathcal{G}(j, i; -\tau) d\tau. \quad (23)$$

Writing the Green function in the representation of eigenvectors $|n\rangle$,

$$\mathcal{G}(i, j; \tau) = \sum_n \psi_n^*(\mathbf{r}_i) \psi_n(\mathbf{r}_j) e^{-(E_n - \mu)\tau} \times \begin{cases} -(1-f(E_n)), & \tau > 0 \\ f(E_n), & \tau < 0 \end{cases}, \quad (24)$$

we find the RKKY coupling between the magnetic impurity spin operators \vec{S}_i, \vec{S}_j ,

$$J_{\text{RKKY}}(\mathbf{r}_{ij}) = J_i J_j \chi_{ij} = J_i J_j \frac{V_a^2}{4\pi} \text{Im} \int dE f(E) \sum_{n,l} \frac{\psi_n^*(\mathbf{r}_i) \psi_n(\mathbf{r}_j)}{E - E_n + i\varepsilon} \frac{\psi_l(\mathbf{r}_i) \psi_l^*(\mathbf{r}_j)}{E - E_l + i\varepsilon}, \quad (25)$$

where $V_a = L^d/N$. Note that often when discussing the RKKY coupling, the magnetic impurity spins are treated classical. Then, the coupling has to be multiplied by $S(S+1)/S^2$ to account for quantum fluctuations of the magnetic impurity spins. Here, we keep the quantum spin operators, since we want to consider the competition with the Kondo effect, for which quantum spin fluctuations are essential. We see that the RKKY coupling depends not only on the local intensities of the conduction electrons $|\psi_n(\mathbf{r}_i)|^2$, but also on the phase difference between the eigenfunctions at the different locations $\mathbf{r}_i, \mathbf{r}_j$. Inserting plane-wave states $\psi_n(\mathbf{r}_i) \sim \exp(i\mathbf{k}\mathbf{r}_i)$ into Eq. (25) one finds at large distances $k_F r_{ij} \gg 1$ the RKKY coupling in d dimensions [30],

$$J_{\text{RKKY}}^0(\mathbf{r}_{kl}) \rightarrow -c_d N_0 J_i J_j \sin(2k_F r_{ij} + d\pi/2) \frac{V_a}{r_{ij}^d}, \quad (26)$$

with $r_{ij} = |\mathbf{r}_i - \mathbf{r}_j|$, k_F the Fermi wave number, $V_a = V/N$, $c_{d=2} = 1/\pi$, $c_{d=3} = 1/(2\pi)$, and $N_0 = 1/D$. Here, $N_0 = V_a \rho_0/2$ is the number of states per energy and spin with total density of states (including the factor 2 for spin) $\rho_0 = m/\pi$ in $d = 2$ dimension and $\rho_0 = mk_F/\pi^2$ in $d = 3$, where m is the effective electron mass. In Fig. 3 results for the coupling between two magnetic adatoms on a metal surface are plotted for various distances r , as extracted from spin dependent scanning tunnelling microscopy measurements [31].

5 Spin competition: the Doniach diagram

Knowing the Kondo temperature T_K and the RKKY coupling we can now study their competition as function of the local exchange coupling J and the concentration of magnetic moments n_m . The amplitude of the oscillatory RKKY coupling Eq. (26) can be rewritten as $J_{\text{RKKY}}^0/D = c_d J^2 n_m$. Noting that the coupling is dominated by nearest neighbored magnetic moments, we wrote it in terms of the density of magnetic moments $n_M = V_a/R^d$, where R is the average distance between next neighbored magnetic moments. In Fig. 4 (left) we plot both energy scales in $d = 3$ dimensions. For the RKKY-coupling we plot it both for a dense system of magnetic impurities $n_M = 1$ (blue), and for a more dilute case, $n_M = 0.5$ (dashed blue).

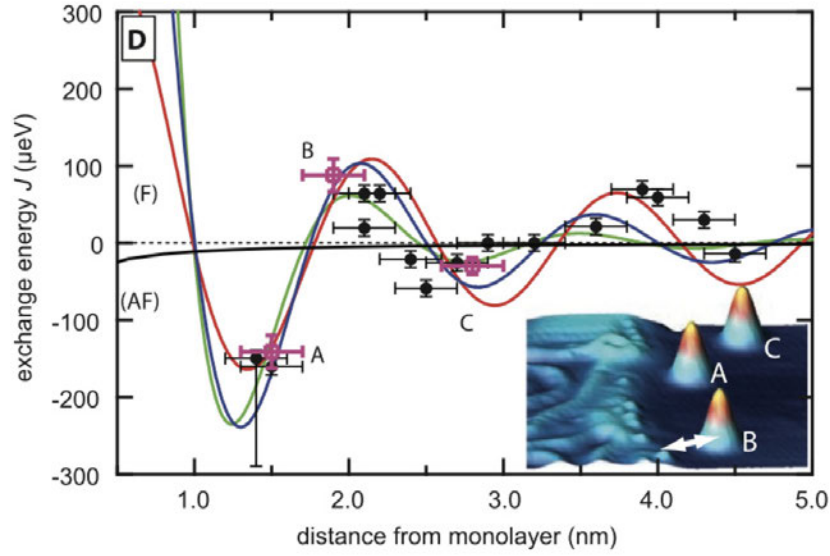


Fig. 3: Magnetic exchange interaction between adatoms on a monolayer stripe. Dots show the measured exchange energy as function of the distance from the monolayer, indicated in the inset. Lines are fits to the 1D, 2D and 3D RKKY-coupling Eq. (26). Figure taken from Ref. [31].

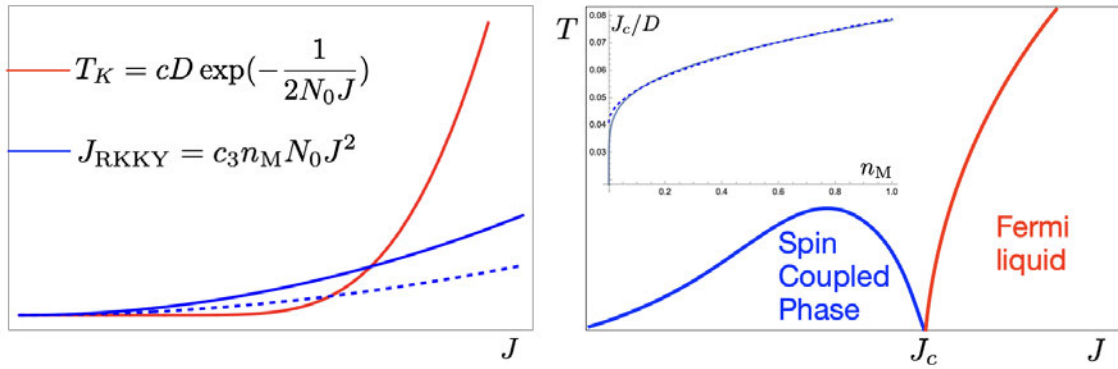


Fig. 4: Left: Kondo temperature T_K with $c = 0.57$ (red) and RKKY coupling J_{RKKY} with $c_3 = 1/(2\pi)$ for (dense, dilute) magnetic impurities, $n_M = (1, 0.5) \equiv$ (blue, blue dashed) as function of exchange coupling J . Right: Doniach diagram, qualitative sketch of transition temperature to a spin coupled state (blue), and to the low temperature Fermi liquid (red), as function of J . The critical coupling J_c/D , Eq. (27), is plotted in the inset as function of magnetic moment density n_M (blue line), together with the fit $J_c/D \approx 0.041 + 0.038\sqrt{n_M}$ (dashed blue).

Thus, we see that there is a critical coupling J_c below which the RKKY coupling exceeds the energy scale for Kondo screening T_K , so that the magnetic impurity spins can be coupled with each other. That critical coupling J_c is seen to increase with the concentration of the magnetic moments. Solving the nonlinear equation analytically, we find

$$J_c = -\frac{D}{4W(-1, -\sqrt{(c_d/c)n_M}/4)}, \quad (27)$$

where $W(k, z)$ is the k -th branch of the Lambert W -function, also known as ProductLog-function, plotted for $d = 3$ in the inset of Fig. 4 (right), blue line. We find for the whole range of concentrations $0 < n_M < 1$, $J_c/D \approx 0.041 + 0.038\sqrt{n_M}$ a good fit (dashed blue line).

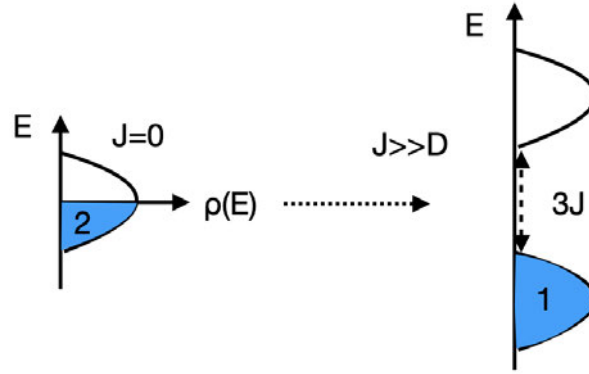


Fig. 5: *Left: Sketch of typical density of states $\rho(E)$ of a metal as function of energy E . The band of width D is half filled with N electrons (blue). Each state is doubly spin degenerate as indicated by 2. Right: Density of states in the presence of a lattice of N magnetic moments, coupled by strong antiferromagnetic exchange coupling $J > D$ to the conduction electron spins, forming N non degenerate Kondo singlet states, as indicated by 1, thereby enlarging the Fermi surface. There is a charge transfer gap $3J$, making that system for $J > D$ a Kondo insulator.*

Doniach argued in Ref. [13] that the critical coupling J_c marks a quantum phase transition between a heavy fermion state and an ordered, typically antiferromagnetic, phase in the Kondo lattice limit $n_M = 1$, where nearest neighbor RKKY coupling is antiferromagnetic. This gives a good description of quantum phase transitions in heavy fermion materials that contain rare earth elements like Ce, Sm, and Yb or actinides like U and Np, where local magnetic moments originate from localized f -orbitals and antiferromagnetic order is observed at sufficiently low temperature. As pressure or external magnetic field is changed, the Néel temperature T_N reaches a maximum, before it is suppressed at the quantum critical point. This has been measured in detail for Cerium compounds, such as CeAl₂, CeAg or CeRh₂Si₂, as well as in YbRh₂Si₂ under pressure and in a magnetic field [32], for a review see [8].

In order to derive that quantum phase transition at $T = 0K$ one needs to find the ground state of the Anderson model with a finite number of M Anderson impurity sites, Eq. (15) or, alternatively, solve the Kondo model of M impurity spins, Eq. (18) as coupled to the conduction band by the antiferromagnetic exchange couplings $J_j = 4t_j^2/U_j > 0$ at the M impurity sites $j = 1, \dots, M$. In a dense Kondo lattice, where $n_M = 1$, the number of impurity spins M equals the number of occupied conduction band states N .

Let us start by looking at a simpler state, a Kondo insulator, which can, for example, form when the uniform coupling is strong $J=J_j \gg D$, exceeding the conduction band width D . Then, the exchange coupling J is so strong that each impurity spin localizes one of the conduction electrons, so that the ground states is given simply by a product of singlet states, $|\psi_0\rangle = \sum_{j=1}^N |0_i\rangle$, where $|0_i\rangle = (|\uparrow_{di}\rangle|\downarrow_{ci}\rangle - |\downarrow_{di}\rangle|\uparrow_{ci}\rangle)/\sqrt{2}$, is the singlet state formed by the impurity spin (indexed by d) and a conduction electron spin (indexed by c) at site i . The ground state energy is then given by $E_0 = -N(3/2)J$. The lowest spin excitation energy gap ΔE_s is obtained by exciting one of the spin pairs to a triplet state of energy $J/2$, thus $\Delta E_s = 2J$. However, there is also a finite charge transfer gap ΔE_q , which is obtained by transferring one of the conduc-

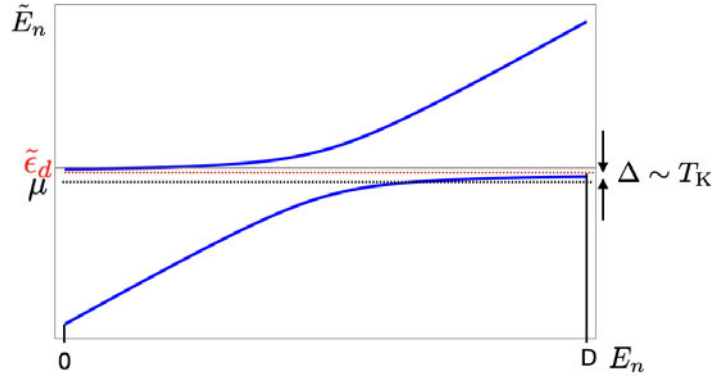


Fig. 6: Quasi particle eigenenergies \tilde{E}_n as function of bare eigenenergies without Kondo coupling E_n . μ is the chemical potential, the energy level of the localized level becomes shifted upward into the gap, $\tilde{\epsilon}_d$. The indirect gap Δ is of the order of T_K ,

tion electrons from site i to site j . Consequently, at site i the impurity spin is left alone $|\uparrow_{di}\rangle$, breaking up the singlet state $|0_i\rangle$, and shifting its energy to $E_i = 0$, while at site j the singlet state is also broken up to accommodate the second electron, exciting the state to $|\uparrow_{di}\rangle|\downarrow_{ci}\rangle|\uparrow_{ci}\rangle$, with energy $E_j = 0$, since the spins of the two conduction electrons compensate each other to $s_{\text{tot } j} = 0$, so that the magnetic impurity spin at site j cannot couple to them. As a consequence, a transfer of a single electron from site i to site j costs in total $\Delta E_q = 2(3/2)J$. Thus, the exchange coupling J to localized magnetic moments prevents charge transfer, opening a large gap $\Delta E_q = 3J$. Taking into account the finite band width D due to the dispersion of the conduction electrons, each of the N Kondo singlets is formed rather by electrons in superpositions of conduction band states. Thus, these Kondo clouds overlap strongly in space. To accommodate all N conduction electrons in these N Kondo singlets, the Fermi surface expands to embrace all states in the conduction band, as compared to the half filled conduction band with doubly occupied states, which is the ground state without the exchange coupling J , see Fig. 5 and the discussion in Refs. [7, 8]. Above this ground state of Kondo singlets, the gap $\Delta E_q = 3J$ opens, the energy needed to transfer one electron from one Kondo singlet to another, making the system an insulator. In fact, this is the mechanism for the formation of a Kondo insulator, which has been experimentally observed, first in SmB_6 [33].

When the exchange coupling is smaller than the band width $J < D$, the ground state is no longer a simple product of Kondo singlets. One way to derive the ground states then is by a mean-field treatment of a generalized Kondo lattice Hamiltonian with degeneracy $N_K \gg 1$, the Coqblin-Schrieffer Hamiltonian [34], performing a $1/N_K$ -expansion, as done first in Refs. [35] and [36]. Thereby one finds the quasi particle eigenenergies \tilde{E}_n as function of the eigenenergies of the conduction band without Kondo coupling, E_n ,

$$\tilde{E}_n = \frac{1}{2}(E_n + \tilde{\epsilon}_d) \pm \frac{1}{2}\sqrt{(E_n - \tilde{\epsilon}_d)^2 + 4V^2}. \quad (28)$$

as plotted in Fig. 6 as function of E_n . Thus, there opens a gap $\Delta = T_K$, relating the mean-field order parameter V to the Kondo temperature T_K by $4V^2 = DT_K$, when $\tilde{\epsilon}_d \approx D/2$. The density of states above and below the gap is seen to be strongly enhanced. The chemical potential is located in the lower band, so that the exchange coupling transformed the Fermi sea

of conduction electrons to a Fermi sea of heavy holes. The energy level of the localized level ε_d becomes shifted upward into the gap, $\tilde{\varepsilon}_d$. With the invention of dynamical mean-field theory, exploiting the fact that mean-field theory becomes exact in infinite dimension $d \rightarrow \infty$ [37], another route to solve the Kondo lattice model and the periodic Anderson model opened, which allows the calculation of self energies [38, 39] and of the resistivity. Thereby, the decay of the resistivity was shown as coherent heavy fermions form at low temperature [40], in agreement with experiments on heavy fermion compounds, as reviewed above.

However, in order to allow the study of the competition between the Kondo screening and the RKKY-coupling both approaches need to be modified. By adding the RKKY-coupling between the magnetic moments to the Kondo lattice hamiltonian, the quantum phase diagram can be studied in mean-field theory, when combined with the $1/N_K$ -expansion [41–44].

A system of two magnetic impurities in a metal has been studied in detail with nonperturbative methods like the numerical renormalization group [45–49]. Such a system has also been realized experimentally by Co atoms on a gold surface and studied varying their distance with scanning tunnelling microscopy [50]. One finds a crossover between a state where both magnetic moments are Kondo screened by the conduction electrons and a state where the impurity spins are coupled. Depending on their distance, they form either a singlet, enforced when RKKY coupling is antiferromagnetic, or a triplet state, when the coupling is ferromagnetic. Building on these studies, DMFT has been extended to Cluster-DMFT, where the exact results for a cluster of few spins, in particular two magnetic impurities are used to enhance the DMFT and to derive the phase diagram of the Kondo lattice model with RKKY coupling [51].

Further insights into this competition comes from exact analytical results for the 1D Kondo lattice and the 1D periodic Anderson model employing the bosonization technique, see Refs. [52] and [53] and references therein. At half filling a Kondo insulator is found, and both the spin and charge transfer gaps have been derived [52].

Recently, Nejadi *et al.* extended the renormalization group equations for a Kondo lattice incorporating self consistently the RKKY coupling between magnetic moments [54]. Thereby they could show that the Kondo temperature is decreased as the exchange coupling J is decreased, as found with diagrammatic methods in Refs. [55–57]. Furthermore, it was found in Ref. [54] that the Kondo screening is quenched at a critical coupling J_c . Since this approach to the spin competition problem is very insightful let us review it in the remainder of this section.

The renormalization of the effective coupling $\tilde{J}(\Lambda)$ at energy Λ , above and below the Fermi energy, Eq. (10), is modified by the RKKY coupling as derived first in Ref. [54] and generalized in Ref. [58] to account for an energy dependent local density of states $\rho(E, \mathbf{r}_i)$, yielding

$$\begin{aligned} \frac{d\tilde{J}_i}{d \ln \Lambda} = & -\tilde{J}_i^2 \frac{V_a}{2} \sum_{\alpha=\pm} \rho(\mu+\alpha\Lambda, \mathbf{r}_i) \\ & + \frac{4}{\pi} \tilde{J}_i^2 J_i^0 \sum_{\alpha=\pm} \sum_{j \neq i} J_j^0 \text{Im} \left(e^{i\mathbf{k}_F \mathbf{r}_{ij}} \chi_c(\mathbf{r}_{ij}, \mu+\alpha\Lambda) G_c^R(\mathbf{r}_{ij}, \mu+\alpha\Lambda) \chi_f(\mathbf{r}_j, \mu+\alpha\Lambda) \right), \end{aligned} \quad (29)$$

where Λ is the effective band cutoff for the renormalization group flow. While the first term on the right hand side is the well known 1-loop RG for the Kondo problem with energy de-

pendent density of states, Eq. (10) [18, 20], the second term describes the correction due to RKKY-coupling. Here, $\chi_f(\mathbf{r}_j, E)$ is the spin susceptibility of the magnetic moment at site \mathbf{r}_j . $G_c^R(\mathbf{r}_{ij}, E)$ is the retarded conduction electron propagator from site \mathbf{r}_i to \mathbf{r}_j and we defined the distance vector $\mathbf{r}_{ij} = \mathbf{r}_i - \mathbf{r}_j$. $\chi_c(\mathbf{r}_{ij}, E)$ denotes the conduction electron correlation function between sites \mathbf{r}_i and \mathbf{r}_j . Solving Eq. (29) we can thus derive the position dependent Kondo temperatures for a given configuration of magnetic moments.

When the magnetic moment density n_M is not too large, $\chi_f(\mathbf{r}_j, E)$ can be approximated by the Bethe-Ansatz solution for a single Kondo impurity [23, 24]. In Ref. [54] this approximation has been used. Then, only its real part contributes, as given by $\text{Re } \chi_f(\mathbf{r}_j, \mu + D) = \mathcal{W}/(\pi T_{Kj} \sqrt{1 + D^2/T_{Kj}^2})$. Here, \mathcal{W} is the Wilson ratio. T_{Kj} is the Kondo temperature at site \mathbf{r}_j . Since it is well known that the energy dependence of the density of states changes the Kondo renormalization [59], it is in general important to keep the energy dependence of all functions and not to replace it with their value at the chemical potential, when the density of states is strongly varying with energy, as in the presence of a pseudo-gap, or in disordered systems.

But, let us first consider the simpler case of magnetic moments in a clean metal, with slowly varying density of states. Then, we can furthermore assume that all conduction electron properties, the local density of states, the propagator $G_c^R(\mathbf{r}_{ij}, E)$ and the correlation function $\chi_c(\mathbf{r}_{ij}, E)$ depend only weakly on energy, and therefore can be replaced by its value at the chemical potential μ , as has been done in Ref. [54]. Then, we can define the effective Kondo coupling $g_i = N(\mu)J_i$ of the Kondo impurity at site \mathbf{r}_i , where $N(\mu) = V_a\rho(\mu)/2$, and find the renormalization group equation for g_i , as modified by the RKKY coupling [54],

$$\frac{dg_i}{d \ln \Lambda} = -2g_i^2 \left(1 - y_i g_0^2 \frac{D}{2T_K} \frac{1}{\sqrt{1 + (\Lambda/T_K)^2}} \right), \quad (30)$$

where D is the bare bandwidth and $g_0 = N(\mu)J^0$ is the bare, unrenormalized Kondo coupling, y_i is the effective dimensionless RKKY interaction strength at site \mathbf{r}_i , given by [54]

$$y_i = -\frac{8W}{\pi^2 \rho(\mu)^2} \text{Im} \sum_{j \neq i} e^{i\mathbf{k}_F \mathbf{r}_{ij}} G_c^R(\mathbf{r}_{ij}, \mu) \Pi(\mathbf{r}_{ij}, \mu), \quad (31)$$

where W is the Wilson ratio as determined by the Bethe Ansatz solution of the Kondo problem [23, 24]. $G_c^R(\mathbf{r}_{ij})$ is the single particle propagator in the conduction band from site \mathbf{r}_i to \mathbf{r}_j . The summation is over all other magnetic moments at positions \mathbf{r}_j . $\Pi(\mathbf{r}_{ij}, \mu)$ is the RKKY correlation function of conduction electrons between sites \mathbf{r}_i and \mathbf{r}_j . y_i is found to be always positive [54], while the RKKY correlation function can be positive or negative.

It is interesting to observe that the effective Kondo interaction renormalized by the RKKY interaction is a function of Λ/T_K , where Λ is the renormalization group energy scale and T_K is the renormalized Kondo temperature to be determined self-consistently.

For two magnetic moments in a clean system, where the bare couplings g_0 are the same at both sites, and $y_i = y$, one can solve this differential equation to obtain [54]

$$\frac{1}{g} - \frac{1}{g_0} = 2 \ln \frac{2\Lambda}{D} - yg_0^2 \frac{D}{2T_K} \ln \frac{\sqrt{1 + (\Lambda/T_K)^2} - 1}{\sqrt{1 + (\Lambda/T_K)^2} + 1}. \quad (32)$$

When the energy scale Λ coincides with the Kondo temperature, i.e., $\Lambda \rightarrow T_K$, the correction to the effective Kondo interaction is large. Therefore, setting $g(T_K) = \infty$ we get the self-consistent equation for the effective Kondo temperature as a function of the RKKY interaction,

$$T_K(y, g_0) = T_K^0(g_0) \exp\left(-yk g_0^2 \frac{D}{T_K(y)}\right), \quad (33)$$

where $T_K^0(g_0) = cD \exp(-1/(2g_0))$ is the bare Kondo temperature in the absence of the RKKY interaction and the numerical constant is $k = \ln(\sqrt{2} + 1)$. Its solution is

$$T_K(y, g_0) = -\frac{yk g_0^2}{W(-yk g_0^2 / T_K^0(g_0))}, \quad (34)$$

for $y < y_c$ with the critical coupling [54]

$$y_c = T_K^0 / (k e g_0^2 D). \quad (35)$$

Noting that the coupling y is related to the magnetic moment density as $y \sim n_M$, and that $g_0 = N_0 J$, we find that the exchange coupling has to exceed the critical coupling $J_c(n_M)$. Thus, it agrees with the result obtained above, when using the Doniach argument, Eq. (27), up to a numerical constant of order 1. As the exchange coupling J is diminished towards that critical value, J_c , the Kondo temperature T_K becomes diminished continuously, as plotted in Fig. 7. At the critical value, however, it is found to take a finite value $T_K^* = T_{Kc}(J_c) = e^{-1} T_K^0(J_c)$, about one third of its value without the RKKY coupling, before it jumps to zero at smaller J .

For two magnetic Co atoms on a gold surface such a suppression of T_K was observed experimentally in Ref. [50] at varying distance R , as measured in the width of the tunnelling peak with scanning tunnelling microscopy [50]. In that case, one finds a crossover between a state where both magnetic moments are Kondo screened by the conduction electrons and a state where the impurity spins form a singlet, enforced when RKKY coupling is antiferromagnetic.

Applying that to a system of dense magnetic moments, like heavy fermion materials, this result is remarkably different from the Doniach diagram, Fig. 4, where it was assumed that both the Kondo temperature and the critical temperature T_c on the spin coupled side of the transition would decay continuously towards the critical point J_c . However, to conclude on the nature of the quantum phase diagram one would have to include self consistently the change in the spin polarization function in the derivation due to an ordering transition of the unscreened or partially screened magnetic moments or by a spin wave instability of the conduction electrons. The result Eq. (34) also implies that by taking into account the RKKY-coupling, the Kondo temperature becomes dependent explicitly on the distance R between the magnetic moments, and thereby on the density of magnetic moments n_M .

However, when the magnetic impurity concentration n_M is lowered, not only is $J_c \sim \sqrt{n_M}$ diminished, and thereby the parameter range of the ordered phase reduced, but the positions of magnetic moments become distributed randomly. Thus, for $n_M < 1$, the distance between magnetic moments R is random. Thereby, both the sign and amplitude of the RKKY coupling is randomly distributed. This may give rise to the appearance of a richer quantum phase diagram with a spin coupled phase without long range order, such as a *spin glass* state [60], which

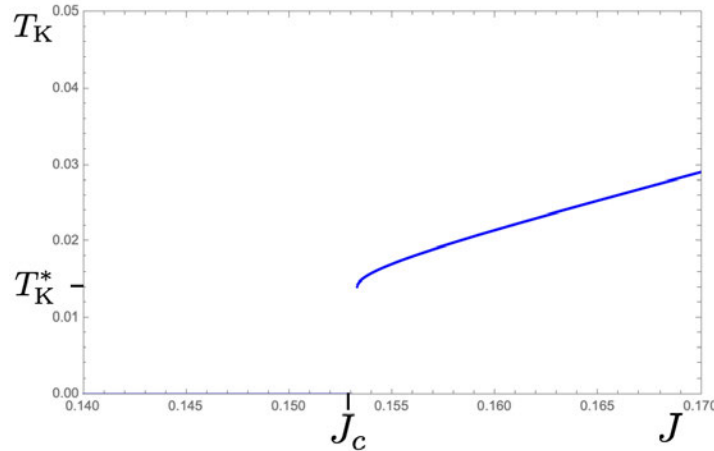


Fig. 7: Kondo temperature as function of J in units of D , $T_K(J)$, Eq. (34), as modified by RKKY coupling for $y = 0.6/k < y_c$. Note that $T_K(J)$ jumps discontinuously from T_K^* to zero at J_c .

competes with an ordered state [41]. In metal wires with dilute magnetic impurities, such as $\text{Ag}_{1-x}\text{Mn}_x$, a transition from a Kondo phase to a spin glass phase has been detected in transport experiments, as the Mn concentration x is enhanced [61]. Spin glass phases have also been found in alloys with rare earth elements, such as $\text{CeNi}_{1-x}\text{Cu}_x$ [62], where the competition between Kondo and RKKY coupling is studied as function of x : CeCu ($x=1$) is at low temperature an antiferromagnet and the alloy remains one up to $x = 0.7$, while CeNi ($x=0$) is a heavy fermion material. Thus, lowering x corresponds to an increase of the local Kondo coupling J , inducing a Doniach like quantum phase transition. However, at intermediate values of x , disorder is relevant, and spin glass behavior is found [62], as reviewed and modelled in [44]. Similar successions of quantum phase transitions between heavy fermion, spin glass and ordered phases have been found in $\text{CeRh}_x\text{Pd}_{1-x}$ as function of x [63]. We will consider the effect of disorder on the competition between Kondo screening and RKKY coupling in section 7, where we will find that new effects introduced by randomness, like Anderson localization and multifractality have to be taken into account in strongly disordered systems with magnetic moments, which profoundly change the quantum phase diagram.

In the next section we consider the effect of a strongly varying density of states on both the Kondo screening and the RKKY-coupling and thereby on the quantum phase diagram.

6 Spin competition in presence of a spectral (pseudo) gap

In semiconductors and insulators the density of states at the Fermi energy is vanishing. At first sight, Eq. (14) seems to imply, that the Kondo temperature is vanishing in such a situation, when $\rho(\varepsilon_F) = 0$. However, the assumption of a smooth density of states is no longer valid and we need to start from the general self consistency equation, Eq. (9). We find that the Kondo effect occurs provided the exchange coupling J exceeds a critical value J_c . Let us review the derivation of the Kondo temperature and J_c for two generic cases when the Fermi level is in a pseudogap and when it is in a hard band gap.

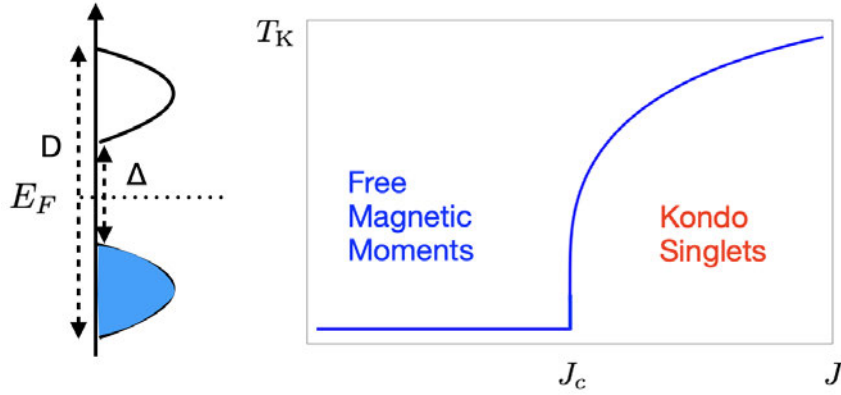


Fig. 8: Left: Schematic density of states with gap Δ , total bandwidth D , Fermi energy E_F in the middle of the gap. Right: Kondo temperature $T_K(J)$ as function of J in units of D , Eq. (38). Note that it decays continuously to zero at the critical coupling $J_c(\Delta)$. Eq. (37).

6.1 Band insulator, semiconductor

Here, we derive the Kondo temperature in a band insulator with a gap Δ , where the Fermi level is in the middle of the gap, as sketched in Fig. 8(left), by inserting the gapped density of states into Eq. (12). For a small gap $\Delta < T_K$, assuming that the density of states is constant and the same in the upper and lower band, ρ_0 , the functional dependence of the Kondo temperature on the exchange coupling J remains the same as in a metal, $T_K \approx c(\Delta) \exp(-1/(2N_0J))$, where N_0 is the number of states per energy and spin, but the pre-factor $c(\Delta) < c$ is diminished compared to a metal, $c = c(\Delta=0) \approx 0.57$. When the gap is larger $\Delta > T_K$, the functional dependence on J changes. Integration of Eq. (12), using that $\tanh(x) \approx 1 - 2 \exp(-2x)$ for $x > 1$, we find the Kondo temperature as a solution of the equation

$$\frac{\Delta}{4} \left(\ln \frac{D}{\Delta} - \frac{1}{2N_0J} \right) = T_K \exp\left(-\frac{\Delta}{T_K}\right). \quad (36)$$

We see that, only when the left side is positive, there can be a real solution for T_K . Thus, the Kondo temperature can only be finite when $J > J_c(\Delta)$, with critical exchange coupling

$$J_c^\Delta = \frac{1}{2N_0} \frac{1}{\ln(D/\Delta)}. \quad (37)$$

As $J \rightarrow J_c^\Delta$ the Kondo temperature is found to decay continuously to zero as

$$T_K = \frac{\Delta}{2} \frac{1}{W(4N_0J/(J/J_c^\Delta - 1))}. \quad (38)$$

For $J \gtrsim J_c^\Delta$ that decay can be approximated as $T_K \approx \Delta/2 / \ln(4N_0J/(J/J_c^\Delta - 1))$. Thus, for $J > J_c^\Delta$ magnetic moments are Kondo screened for temperatures below $T_K(J)$, in spite of the large band gap $\Delta > T_K$. For $J < J_c^\Delta$ all magnetic moments remain unscreened.

Since RKKY couplings, Eq. (25), are dominated by the density of states at the Fermi energy, in an insulator they are small and decay exponentially with distance R . However, when an insulator or semiconductor is doped, there exist other forms of magnetic coupling between magnetic

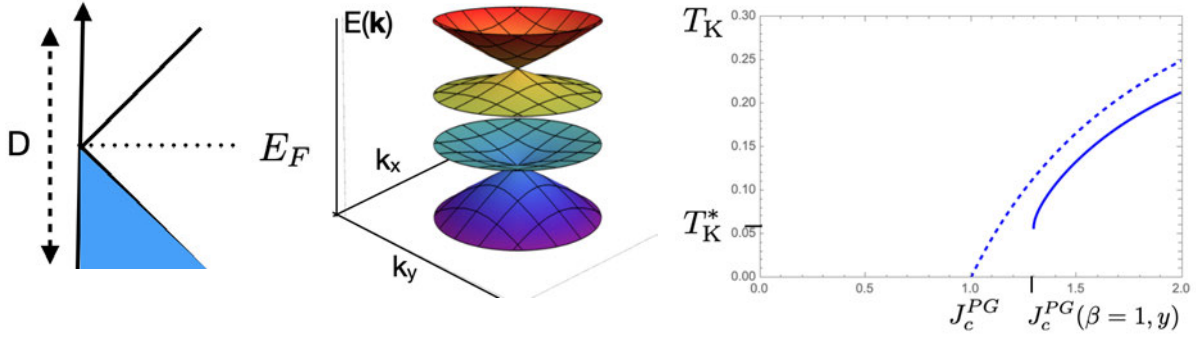


Fig. 9: Left: Schematic density of states with pseudo-gap at Fermi energy E_F , bandwidth D . Middle: Quasiparticle dispersion of a 2D honeycomb Kondo lattice. Fig. taken from Ref. [72]. Right: Kondo temperature in the presence of a pseudo-gap with power $\beta = 1$ with RKKY coupling $y = 1/(32k)$ Eq. (44) (full line) and without, Eq. (40) (dashed line). The Kondo temperature in the presence of RKKY coupling y terminates at the critical coupling Eq. (43) $J_c^{PG}(\beta=1, y) > J_c^{PG}(\beta=1)$, Eq. (39) at the value T_K^* , Eq. (45) and jumps then to zero.

dopants. For spin- $1/2$ dopants, like P in Si, they are known to be coupled by antiferromagnetic superexchange interaction, caused by the overlap of dopant eigenfunctions. Then, dopant spins are in a random singlet state for dilute doping [64], see Ref. [65] for a review. But there can be other exchange mechanisms in dilute magnetic semiconductors, for example the Zener's double exchange coupling and the p - d coupling, which are ferromagnetic. See Ref. [66] for a review.

6.2 Pseudo-gap semimetal

A pseudo-gap opens at the Fermi energy when the density of states vanishes at the Fermi energy as $\rho(E) \sim |E - E_F|^\beta$ with a power $\beta > 0$, as shown schematically in Fig. 9 (left). This occurs in numerous materials, like at the surface of topological insulators [67] and in graphene [68], where the electrons are confined to a 2-dimensional honeycomb lattice. The low-energy excitations in graphene are fermionic quasiparticles described by relativistic massless Dirac fermions, as characterized by a linear dispersion relation, with two Dirac points, where the density of states vanishes linearly with energy ($\beta=1$). Thus, the question arises, what happens when these massless fermions are coupled to local magnetic moments. The answer depends strongly on the magnitude of the exchange coupling J . Plugging in the pseudo-gap density of states $\rho(E) = \rho_0 |(E - E_F)2/D|^\beta$ in the equation for the Kondo temperature, Eq. (12), for $E_F = D/2$, we find for $J > J_c^{PG}(\beta)$ with critical exchange coupling

$$J_c^{PG}(\beta) = \beta/(2N_0) = \beta D/2, \quad (39)$$

the Kondo temperature

$$T_K = \frac{D}{2} \left(1 - \frac{J_c^{PG}(\beta)}{J} \right)^{1/\beta}. \quad (40)$$

Note that for $J \gg J_c^{PG}$, Eq. (40) converges to $T_K^0 \sim D/2 \exp(-1/(2N_0J))$, the Kondo temperature in a metal. There is for $J < J_c^{PG}(\beta)$ no Kondo screening, as has been confirmed with non

perturbative methods like the numerical renormalization group method in Refs. [59, 69, 70], and the concentration of free, unscreened magnetic moments $n_{\text{FM}}(J)$ at $T = 0\text{K}$ is a step function, $n_{\text{FM}}(J) = n_{\text{M}}$ for $J < J_c^{\text{PG}}(\beta)$ and zero otherwise.

It has been shown in Ref. [71] with a large N_K -expansion that there is a quantum phase transition in the Kondo lattice on a 2-dimensional honeycomb lattice at critical coupling J_c , even when neglecting the RKKY coupling. Remarkably, the energy dispersion of quasiparticles in such a system with a pseudo-gap has a direct gap, see Fig. 9 [72], where it was shown that the Kondo-insulator gap is observable in the optical conductivity, in stark contrast to the conventional Kondo lattice system where the Kondo-insulator gap is indirect, see Fig. 6. The Dirac cones become duplicated and shifted up and down in energy, respectively, as seen in Fig. 9.

The RKKY coupling in presence of a pseudo-gap at the Fermi energy is shorter ranged,

$$J_{\text{RKKY}}(\mathbf{R}) = \frac{g(\mathbf{R})}{R^{d+\beta}}, \quad (41)$$

where $g(\mathbf{R})$ is an oscillatory, non decaying function of \mathbf{R} which may be anisotropic, depending on the specific lattice. Here, $R = |\mathbf{R}|$. As an example, in a 2D honeycomb lattice like graphene, where there are two sub-lattices A and B , the RKKY coupling is decaying with power $d+\beta = 3$. The oscillatory function is different, when the magnetic moments are placed on the same sub-lattices, as given by [73] $g_{AA}(\mathbf{R}) = -J^2(1 + \cos(\Delta\mathbf{K} \cdot \mathbf{R}))$, while on different sub-lattices, $g_{AB}(\mathbf{R}) = J^2 3(1 - \cos(\Delta\mathbf{K} \cdot \mathbf{R} - 2\vartheta_R))$, where $\Delta\mathbf{K} = \mathbf{K}^\dagger - \mathbf{K}^-$, with $\mathbf{K}^\dagger, \mathbf{K}^-$ the reciprocal lattice vectors of the two Dirac points. ϑ_R is the angle between the armchair direction and the position vector of the magnetic moment on the lattice.

Thus, both Kondo temperature and RKKY coupling are diminished in the presence of a pseudo-gap. This raises the question how the pseudo-gap modifies their competition. As there is no Kondo screening for $J < J_c^{\text{PG}}(\beta) = \beta D/2$, while the RKKY-coupling is finite for all J , magnetic moments couple in that regime. To find out whether RKKY-coupling is dominating the Kondo screening even for larger exchange couplings $J > J_c^{\text{PG}}(\beta)$, we need to solve the RG-equation, Eq. (29) with RKKY interaction with a pseudo-gap. Inserting the density of states $\rho(E) = \rho_0 |(E - E_F)2/D|^\beta$ into Eq. (29) and integration over Λ up to the breakdown of perturbation theory at scale T_K , yields the equation for the Kondo temperature

$$\frac{J_c(\beta)}{J} - 1 + \left(\frac{2T_K}{D}\right)^\beta + k\beta y_\beta J^2 N_0^2 \frac{D}{2T_K} = 0, \quad (42)$$

where $k = \ln(\sqrt{2} + 1)$, y_β the RKKY coupling function as modified by a pseudo-gap with power β , and $J_c^{\text{PG}}(\beta)$ the critical coupling in absence of y_β , Eq. (39).

Let us consider as an example a pseudo-gap with power $\beta = 1$, as it occurs in graphene and on the surface of topological insulators. For $J > J_c^{\text{PG}}(\beta=1, y)$ with critical exchange coupling

$$J_c^{\text{PG}}(\beta=1, y) = J_c^{\text{PG}} \frac{1 - \sqrt{1 - 4\sqrt{ky}}}{2\sqrt{ky}}, \quad (43)$$

where $J_c^{\text{PG}} = J_c^{\text{PG}}(\beta=1, y=0) = D/2$, is the critical coupling when neglecting the RKKY-

coupling, we find the Kondo temperature

$$T_K = \frac{D}{4} \left(1 - \frac{J_c^{PG}}{J} + \sqrt{\left(1 - \frac{J_c^{PG}}{J}\right)^2 - ky \left(\frac{J}{J_c^{PG}}\right)^2} \right). \quad (44)$$

Note that at the critical coupling $J_c^{PG}(\beta=1, y)$ it has a finite value,

$$T_K^* = \frac{D}{4} \left(1 - \frac{J_c^{PG}}{J_c^{PG}(\beta=1, y)} \right), \quad (45)$$

one half of the value it has at that exchange coupling $J_c^{PG}(\beta=1, y) > J_c^{PG}$, without RKKY-coupling. Thus, even in the presence of a pseudo-gap, the Kondo temperature jumps discontinuously to zero at $J_c^{PG}(\beta=1, y)$ as seen in Fig. 9(right), similar to what was found in a metal, Fig. 7. The critical coupling $J_c^{PG}(\beta=1, y)$ is an increasing function of the RKKY-coupling y_1 for $0 < y < 1/(16k)$, varying from $D/2$ to D . For stronger coupling $y > 1/(16k)$ there is no finite Kondo temperature and thus no Kondo screening for any coupling J .

7 Spin competition in the presence of disorder

Any real material has some degree of disorder. In doped semiconductors it arises from the random positioning of the dopants themselves, in heavy fermion materials it may in addition arise from structural defects or impurities caused by atomic defects. Disorder can cause Anderson localization, trapping electrons in the disorder potential. Thus, in order to fully understand the physics of electron systems with magnetic moments, we need to understand how Anderson localization affects the competition between Kondo screening and RKKY coupling, and how that in turn affects Anderson localization. Moreover, as noted already early [74], the physics of random systems is fully described only by probability distribution functions, not just averaged quantities. Thus, for electron systems with randomly located magnetic moments the derivation of physical properties requires the knowledge of distribution functions of both the Kondo temperature and the RKKY coupling [75], not just their averages. In fact, anomalous distributions of the Kondo temperature T_K and the RKKY coupling can give rise to non-Fermi-liquid behavior, as measured for example in the low-temperature power-law divergence of the magnetic susceptibility in doped semiconductors close to the metal-insulator transition [65].

7.1 Distribution of Kondo temperature and RKKY couplings

Since the Kondo temperature depends on the product of the local exchange coupling J and the density of states at the Fermi energy ρ [1, 17, 18], it is natural to expect a distribution of the Kondo temperature, $P(T_K)$, when J and ρ are distributed due to the random placement of the dopants, as has been pointed out in Refs. [74–79].

Indeed, the disorder potential results in wave function amplitudes which vary randomly, both spatially and with energy. In a weakly disordered metal different wave functions are correlated with each other in a macroscopic energy interval of the order of the elastic scattering

rate $1/\tau$. This results already in weakly disordered metals in a Kondo temperature distribution of finite width in the thermodynamic limit [27, 28]. To model the disorder one adds a disorder potential $V(\mathbf{r})$ to the one particle Hamiltonian, which can be assumed to be spatially uncorrelated and white noise distributed with width given by the elastic scattering rate $1/\tau$. Using the 1-loop equation for the Kondo temperature written in terms of the local density of states $\rho(E, \mathbf{r})$, Eq. (12), let us rewrite it in terms of the disorder induced local deviations $\delta\rho(E, \mathbf{r}) = \rho(E, \mathbf{r}) - \langle \rho(E, \mathbf{r}) \rangle$, where $\langle \dots \rangle$ denotes the average over the disorder potential. Denoting $T_K^{(0)}$ as the Kondo temperature obtained with the average local density of states, $\nu = \langle \rho(E, \mathbf{r}) \rangle$ we find the Kondo temperature for a given realization of the disorder potential [20]

$$T_K = T_K^{(0)} \exp\left(\int_0^D dE \frac{\delta\rho(\mathbf{r}, E)}{2\nu(E-E_F)} \tanh\left(\frac{E-E_F}{2T_K}\right)\right). \quad (46)$$

Taking the square of the logarithm of Eq. (46) and

$$\left\langle \ln^2\left(\frac{T_K}{T_K^{(0)}}\right) \right\rangle = \int_0^D dE \int_0^D dE' \left\langle \tanh\left(\frac{E-E_F}{2T_K^{(0)}}\right) \tanh\left(\frac{E'-E_F}{2T_K^{(0)}}\right) \frac{\delta\rho(\mathbf{r}, E)}{2\nu(E-E_F)} \frac{\delta\rho(\mathbf{r}, E')}{2\nu(E'-E_F)} \right\rangle. \quad (47)$$

The disorder averaged correlation function of local density of states $\langle \rho(\mathbf{r}, E) \rho(\mathbf{r}, E') \rangle$ is governed at weak disorder $E_F\tau > 1$ by diffusion and Cooperon modes, as obtained by summing up ladder diagrams, describing multiple elastic scattering of the electrons from the impurity potential. For a review see [80]. Physically, these diffusion modes account for the fact that electrons in a disorder potential do not move ballistically along straight paths, but rather diffusively, such that the average square of the path length $\mathbf{r}(t)$ on which an electron moves within a time t is given by $\langle \mathbf{r}(t)^2 \rangle = D_e t$, where $D_e = v_F^2 \tau / d$, is the diffusion constant. Thereby one finds for the standard deviation of the Kondo temperature in the thermodynamic limit [27, 28]

$$\delta T_K \approx T_K^{(0)} \begin{cases} \frac{c_3}{(E_F\tau)\sqrt{\beta}} \ln\left(\frac{1}{\tau T_K^{(0)}}\right) & \text{in } d = 3, \\ \frac{1}{\sqrt{3\pi E_F\tau\beta}} \left[\ln\left(\frac{1}{\tau T_K^{(0)}}\right) \right]^{3/2} & \text{in } d = 2, \\ 2\sqrt{\frac{\pi\sqrt{3}}{k_F^2 A\beta}} (\tau T_K^{(0)})^{-1/4} & \text{in quasi 1-d wire of cross section } A, \end{cases} \quad (48)$$

with c_3 a constant. Note that it is larger with time-reversal symmetry $\beta = 1$ than when it is broken by a magnetic field $\beta = 2$, which diminishes weak localization corrections. In the weak disorder limit, the Kondo temperature has a Gaussian distribution with width given by Eq. (48). However, its distribution becomes strongly bimodal as disorder is increased further with an increasing weight at small Kondo temperature, see Fig. 10(left), where the distribution of T_K is plotted, obtained numerically for a tight binding model on a square lattice with potential disorder of box distribution and width W [72]. Furthermore, a finite concentration of *free* magnetic moments is found when electrons at the Fermi energy are localized. Since these effects can be explained by Anderson localization and multifractality, we will return to the Kondo temperature distribution after introducing these phenomena in the next chapters.

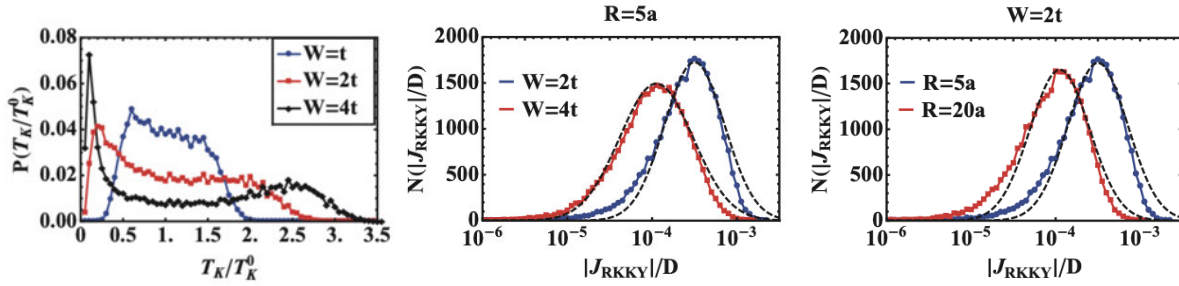


Fig. 10: Left: Distribution of Kondo temperature for different disorder strengths W . Middle: distribution of absolute value of the RKKY coupling at fixed distance $R = 5a$ for different disorder strengths W . Right: at fixed $W = 2t$ for distances $R = 5a, 20a$. Dashed lines: lognormal distribution with fitted parameters. All results are obtained for a 2D tight binding model on a square lattice, with lattice spacing a , with potential disorder, box distribution of width W in units of hopping amplitude t , Fermi energy $E_F = t$. All Figs. taken from Ref. [72].

As the RKKY coupling is mediated by conduction electrons, it is strongly affected by their elastic scattering from the disorder, as well. Indeed, the disorder averaged RKKY coupling decays exponentially for distances larger than the mean free path $l_e = v_F \tau$ [81]. This can be understood from the fact that it depends on the product of the electron wave function amplitudes at the locations \mathbf{r}_i and \mathbf{r}_j , see Eq. (25), and thereby on the electron phase difference between these two locations, which the elastic scattering from disorder randomizes. However, its geometrical average is hardly changed from its value in the clean limit [82–84], which is valid even at stronger disorder, as long as the distance between the magnetic moments is not larger than the localization length. The distribution of the RKKY coupling deviates from a normal distribution already at weak disorder and converges to a log-normal distribution at stronger disorder, $P(x = \ln(|J_{\text{RKKY}}|/D)) = \exp(-(x-x_0)^2/(2\sigma^2))/(\sqrt{2\pi}\sigma)$, with x_0 and σ disorder dependent parameters, as was derived with a field-theoretical approach [85]. That was confirmed numerically for 2D disordered metals in Refs. [86–88], as seen in Fig. 10(middle and right). There, the distribution of $|J_{\text{RKKY}}|$ is plotted as obtained numerically for a tight binding model on square lattice with potential disorder and box distribution of width W for various distances between the magnetic moments R as compared to the lognormal distribution with fitted parameters (dashed lines) [72]. This is expected, since the amplitude of the RKKY coupling, Eq. (25), is dominated by the local density of states at the Fermi energy, which has at strong disorder and close to the Anderson localization transition a lognormal distribution [80]. The width σ of the lognormal distribution has been derived in Ref. [85] to scale with the elastic scattering rate as $1/\tau$ as $\sigma \sim \tau^{-1/2}$, which has been confirmed numerically in 2D disordered systems [88], noting that $1/\tau = \pi W^2/(6D)$ with $D = 8t$ the band width of the 2D tight binding model.

7.2 Anderson localization – local spectral gaps

Disorder can result in Anderson localization, where states are exponentially localized with localization length ξ , forming a discrete spectrum with local level spacing Δ_ξ as sketched in Fig. 11(left). Since electrons need then to be thermally activated to contribute to a current, their resistivity is found at low temperature to increase exponentially. The interplay of Anderson

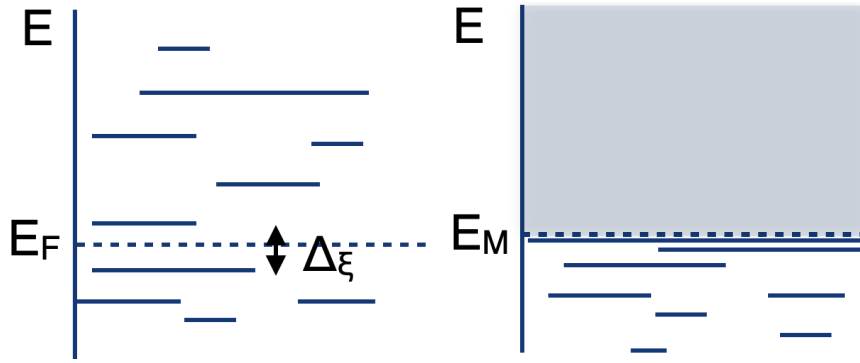


Fig. 11: *Left: Spectrum of localized states with local level spacing Δ_ξ . Right: Spectrum with mobility edge E_M , where for $E < E_M$ all states are localized, while for $E > E_M$ there is a continuum of extended states. At the mobility edge $E = E_M$ there is a critical state.*

localization with spin correlations like Kondo effect and RKKY interaction, has only recently received increased attention, even though both spin correlations and disorder effects are relevant for many materials, including doped semiconductors close to the metal-insulator transition [89,65], and typical heavy Fermion systems like materials with $4f$ or $5f$ atoms [90,44].

In $d = 3$ and higher dimensions mobility edges E_M appear in the band of eigenstates of a Hamiltonian of electrons moving in a disorder potential $V(\mathbf{r})$. Then, the eigenstates are found to be localized with energy dependent localization length $\xi(E)$ at the band edges. There is a delocalization transition at E_M to a continuum of extended states, as sketched in Fig. 11(right), where the localization length diverges with a power law $\xi(E) \sim |E - E_M|^{-\nu}$ with critical exponent ν . For $d < 2$ all states are localized for a Hamiltonian of noninteracting disordered electrons. For $d = 2$ all states are localized in a disorder potential without magnetic field, or in weak magnetic field. In the presence of a strong perpendicular magnetic field in two dimensions, critically extended states appear in the middle of Landau bands, which is known as the integer quantum Hall transition. In presence of spin-orbit interaction in two dimensions there is a critical delocalization transition. Also, long range interactions may cause a delocalization transition in two dimensions. For reviews on Anderson localization, see Refs. [91–97].

When eigenstates are localized with localization length $\xi(E)$, the spectrum is discrete with a local spacing between the energy levels $\Delta_\xi = 1/(\rho(E)\xi(E)^d)$, where $\rho(E)$ is the density of states at energy E and d is the dimension. Thus, when placing magnetic moments in a disordered electron system, and the Fermi energy E_F is in the band of localized states, the Kondo renormalization of exchange couplings stops at energy scale $\Delta_\xi(E_F)$, since there are no states coupling to the magnetic moment at lower energy. Even though the gap is local, as the exchange coupling is local as well, this problem is equivalent to the Kondo effect in the presence of a spectral gap, which we reviewed in section 6. Thus, we can conclude that there is a critical exchange coupling J_c^A below which the magnetic moment remains unscreened, where

$$J_c^A(\Delta_\xi) = \frac{1}{2N_0} \frac{1}{\ln(D/\Delta_\xi(E_F))}, \quad (49)$$

where $N_0 = N(E_F) = V_a \rho(E_F)/2$ is the number of states per energy and spin at the Fermi energy.

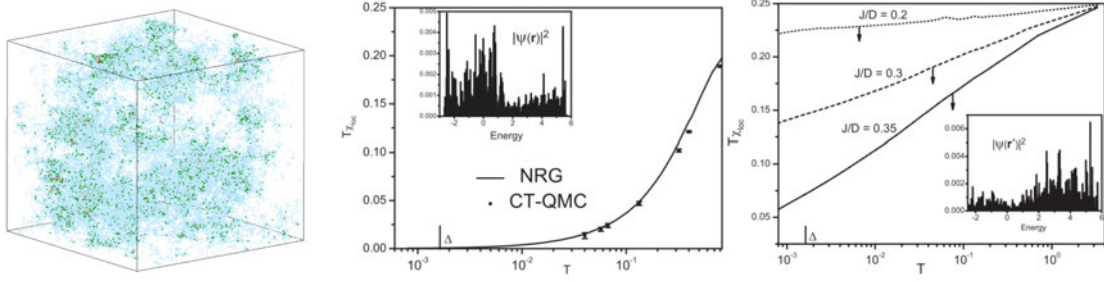


Fig. 12: *Left: Critical state intensity at $E = 2t$ on $d = 3$ Anderson tight binding model ($N = 10^6$ sites, disorder amplitude $W = 16.5t$), obtained by exact diagonalization. Coloring denotes $\alpha = -\ln |\psi|^2 / \ln L$ with $\alpha \in [1.2, 1.8]$ (red), $\alpha \in [1.8, 2.4]$ (green), $\alpha \in [2.4, 3.0]$ (blue). Sites with higher intensity $\alpha < 1.2$ and lower intensity $\alpha > 3$ are not shown. Thereby, 80 % of total state intensity is visible. Fig. taken from Ref. [103]. Middle and Right: Local spin susceptibility as function of temperature T for spin $S = 1/2$ coupled by exchange coupling $J = 0.35D$, disorder amplitude $W = 2t$ in 2D lattice ($L = 70$), obtained with numerical renormalization group (lines) and continuous time quantum Monte Carlo (dots) method, at sites where Kondo temperature T_K is maximal (middle) and where the magnetic moment remains free (right). Arrows indicate $T_K^{(0)}(J)$. Insets: Intensity as function of E ($E_F = 0$). Fig. taken from Ref. [102].*

The RKKY coupling, on the other hand, is cut off for length scales exceeding the localization length at the Fermi energy $R > \xi(E_F)$, but remains finite between magnetic moments whose distance is smaller, $R < \xi(E_F)$. At and in the vicinity of the mobility edge E_M , another phenomenon has to be taken into account, to understand the competition between Kondo effect and RKKY-coupling: there the eigenfunction intensities have multifractal distributions and the intensities at different energy are power law correlated. We give a brief introduction to multifractality in the next chapter, before reviewing its effects on spin correlations.

7.3 Multifractality – local pseudo-gaps

Multifractality has been observed experimentally in disordered thin film systems measuring the local density of states by scanning tunnelling microscopy [98, 99]. In the vicinity of the Anderson delocalization transition wave functions have been shown to be strongly inhomogeneous, multifractal [96] and power law correlated in energy [100, 101]. Since the delocalization transition is a 2nd order quantum phase transition, the localization length ξ on the localized side of the transition, and the correlation length ξ_c on the metallic side, diverge at E_M as $\xi(E) \sim |E - E_M|^{-\nu}$ and $\xi_c(E) \sim |E - E_M|^{-\nu_c}$, where universality implies $\nu = \nu_c$. Thus, at the mobility edge there is a critical state, which is very sparse, but spread over the whole sample, see Fig. 12(left), where the intensity $|\psi_n(\mathbf{r})|^2$ is plotted for all sites of a finite sample of the 3-dimensional tight binding model with onsite disorder potential. The critical eigenfunction intensities $|\psi_l(\mathbf{r})|^2$ are found to scale linearly with size L as,

$$P_q = L^d \langle |\psi_l(\mathbf{r})|^{2q} \rangle \sim L^{-d_q(q-1)}. \quad (50)$$

Critical states are characterized by multifractal dimensions $d_q < d$, smaller than spatial dimension d and changing with power q . The local intensity distribution of a critical state is close to a log-normal distribution function, as given by [96]

$$P(|\psi_l(\mathbf{r})|^2) \sim L^{\alpha_\psi - (\alpha_\psi - \alpha_0)^2 / (2\eta)}, \quad (51)$$

where $\alpha_\psi = -\ln |\psi_l(\mathbf{r})|^2 / \ln L$ and $\eta = 2(\alpha_0 - d)$ with $\alpha_0 > d$. Then, $d_q = d - q(\alpha_0 - d)$ for $q < q_c$. For $q > q_c = \alpha_0 / \eta$ it terminates at τ_{q_c} [96]. Away from criticality wave functions show multifractality at length scales smaller than the localization length $\xi(E)$ and the correlation length $\xi_c(E)$, respectively, where moments scale with $\xi(E)$, $\xi_c(E)$ in multifractal dimensions d_q .

Another consequence of multifractality is that intensities are power law correlated in energy [100, 101] within correlation energy $E_c \sim 1/\tau$. Given that the intensity at the critical energy $E_k = E_M$ is $|\psi_M(\mathbf{r})|^2 = L^{-\alpha_\psi}$ the conditional intensity of a state at energy E_l , is relative to the intensity of an extended state L^{-d} given by [103]

$$I_\alpha = L^d \langle |\psi_l(\mathbf{r})|^2 \rangle_{|\psi_M(\mathbf{r})|^2 = L^{-\alpha_\psi}} \sim \left| \frac{E_l - E_M}{E_c} \right|^{\beta_\alpha}, \quad (52)$$

for $|E_l - E_M| < E_c \sim 1/\tau$. Thus the intensity varies with a power law with power $\beta_\alpha = (\alpha_\psi - \alpha_0)/d$ for $|E_l - E_M| > \Delta$ (when E_l is closer to E_M than the level spacing Δ , the conditional intensity reduces to the intensity itself, $L^{-\alpha_\psi}$). At positions where the intensity is small, $\alpha > \alpha_0$, it remains suppressed within an energy range of order $1/\tau$ around E_M forming a *local pseudo-gap* with power $\beta_\alpha > 0$. Indeed, such local pseudo-gaps are found numerically with only small fluctuations, see the inset of Fig. 12(right) for a 2D disordered system with linear size $L < \xi$ at $E_F = 0$. When the intensity is larger than its typical value $L^{-\alpha_0}$, $\alpha < \alpha_0$, it remains enhanced within an energy range of order $1/\tau$ around E_M , increasing as a power law when E_l approaches the mobility edge. An example of such strong enhancement at $E_F = 0$, as obtained numerically for a 2D system with linear size $L < \xi$, is shown in the inset of Fig. 12(middle). Implementing multifractality and power law correlation of intensities, the Kondo temperature T_K is found by inserting the conditional intensity of state l , Eq. (52) into Eq. (9),

$$1 = \frac{J\Delta}{2DE_c} \sum_{|\varepsilon_l| < E_c} \left| \frac{\varepsilon_l}{E_c} \right|^{\beta_\alpha - 1} \tanh \left(\frac{\varepsilon_l}{2T_K} \right), \quad (53)$$

where the summation over l is restricted to energies within the energy interval of the correlation energy $E_c \sim 1/\tau$ around the mobility edge. The power is given by $\beta_\alpha = (\alpha_\psi - \alpha_0)/d$ for $\Delta < |E_l - E_M| < E_c$. Thus, Eq. (53) defines the Kondo temperature in a system with *pseudo-gaps* of power β_α , in the local density of states when it is positive [59] and the Kondo temperature is reduced at such sites. On the other hand, at sites where β_α is negative T_K is enhanced. Eq. (53) can be solved analytically yielding [103]

$$\frac{T_K}{E_c} = \left[\left(1 - \frac{J_c^{PG}(\beta_\alpha)}{J} \right) c_\alpha \right]^{\frac{1}{\beta_\alpha}}, \quad (54)$$

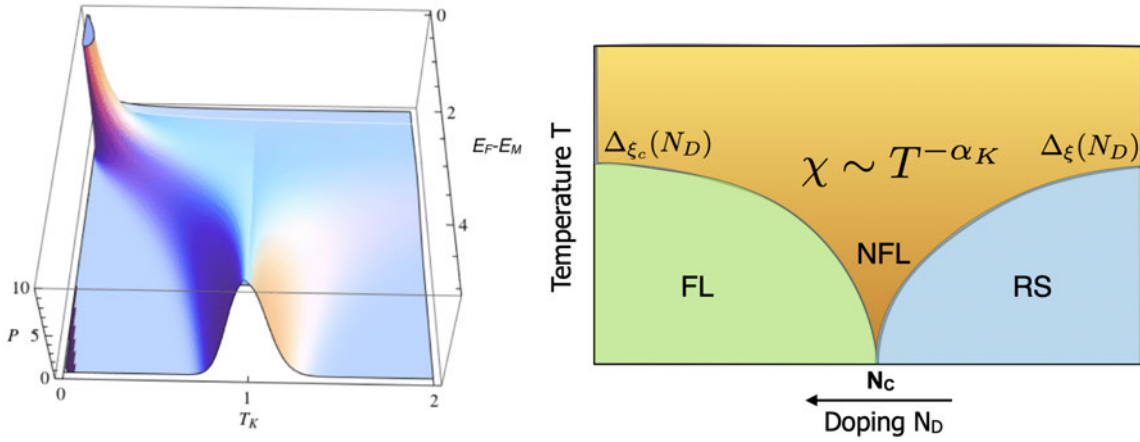


Fig. 13: Left: Kondo temperature T_K -distribution in units of $T_K^{(0)}$ as function of distance to the mobility edge $E_F - E_M$ in units of E_c for exchange coupling $J = D/5$, derived analytically. Fig. taken from Ref. [103]. Right: Schematic phase diagram as function of doping concentration N_D , near critical doping N_c . Non-Fermi liquid behavior at temperatures exceeding the scale $\Delta_{\xi_c}(N_D)$ on the metallic side and $\Delta_{\xi}(N_D)$ below which there is a Fermi liquid (FL) due to Kondo screening, and a random singlet state (RS), respectively.

where $\beta_\alpha = (\alpha_\psi - \alpha_0)/d$, and the critical exchange coupling is $J_c^{PG}(\beta_\alpha) = \beta_\alpha D/2$ and $c_\alpha = (2\alpha_\psi - \eta)/(\alpha_\psi - \eta/2 + d)$. Thus, the Kondo temperature has the form we found in the presence of a pseudo-gap Eq. (40), with power β_α . For $J < J_c^{PG}(\beta_\alpha)$ the magnetic moment remains unscreened. Since $\alpha_\psi \in [0, \infty]$ is distributed, we find that $J_c^{PG}(\beta_\alpha)$ and thereby $T_K(\alpha)$ are distributed, accordingly. For the typical value $\alpha_\psi = \alpha_0$ we recover T_K of a clean system $T_K(\alpha_\psi = \alpha_0) \sim E_c \exp(-1D/(2J)) \sim T_K^{(0)}$. The derivation can be extended into the vicinity of the mobility edge, where the (localization, correlation) lengths (ξ, ξ_c) are finite, respectively by substituting in α_ψ the system size L by (ξ, ξ_c) . Thereby, using a normal distribution of α_ψ , the distribution of the Kondo temperature can be derived analytically, as plotted in Fig. 13(left) [103] as function of energy distance to the mobility edge E_M . It evolves from a Gaussian distribution with finite width in the weakly disordered metal regime to a bimodal distribution with a divergent power law tail at the mobility edge. The enhanced weight at low Kondo temperatures was shown in Ref. [103] to originate from the opening of the local pseudo-gaps and is given by

$$P(0 < T_K \ll T_K^0) \sim T_K^{-\alpha_K}, \quad (55)$$

with universal power $\alpha_K = 1 - \eta/(2d)$, with multifractal correlation exponent $\eta = 2(\alpha_0 - d)$. The magnetic susceptibility $\chi(T) \sim n_{FM}(T)/T$ with density of free moments $n_{FM}(T) = n_M \int_0^T dT_K P(T_K)$, at temperature T is found at the mobility edge as [103],

$$\chi(T) \sim \left(\frac{T}{E_c}\right)^{-\alpha_K}, \quad (56)$$

diverging with a universal power law, in good agreement with experimentally observed Non-Fermi liquid behavior in the magnetic susceptibility and specific heat [89] to which the magnetic

moments contribute $C(T) \sim T dn_{FM}(T)/dT$ as $C(T) \sim T^{\eta/(2d)}$. This result is also valid on the insulating side for $T > \Delta_\xi$ and on the metallic side for $T > \Delta_{\xi_c}$, yielding the phase diagram shown in Fig. 13(right) with a Non-Fermi liquid fan, caused by the distribution of Kondo temperatures due to the multifractality in the vicinity of the mobility edge.

Numerical calculations of the T_K -distribution confirm the anomalous power [79, 104] with a power which is very close to the analytical result Eq. (55). In Ref. [102] the magnetic susceptibility was obtained by a full Wilson renormalization group (RG) calculation [21] for a 2D disordered system finding the anomalous power law divergence, shown in Fig. 12 at sites where the intensity is suppressed as in a local pseudo-gap. Recently, it was pointed out that a more realistic model of the Kondo impurity which takes into account anisotropies yields a modified distribution of Kondo temperatures [105]. It remains to be explored whether this will affect the low T_K tail at the AMIT and thereby the anomalous power of the magnetic susceptibility α_K .

On the insulating side of the transition there remains a finite density of magnetic moments in the low temperature limit, since the Kondo screening becomes quenched by Anderson localization, where renormalization of the Kondo coupling becomes cutoff by the local level spacing $\Delta_\xi = 1/(\rho\xi^3)$ [106]. Since these free moments are still weakly coupled to the electron system, they interact with each other in the vicinity of the mobility edge by RKKY-like exchange interactions, extending up to distances of the order of the localization length ξ . In the dilute doping limit the indirect exchange interaction becomes the superexchange interaction due to the overlap of hydrogen like impurity states, which is known to be antiferromagnetic. These randomly positioned magnetic moments have been modelled by a Heisenberg spin model with random antiferromagnetic short range, exponentially decaying exchange interaction [64]. In agreement with experiments, numerical simulations and the implementation of a cluster renormalization group, no evidence for a spin glass transition, at which the magnetic susceptibility would peak and then decay to lower temperatures is found [64]. Rather, the magnetic susceptibility diverges at low temperature with a power law $\chi(T) \sim T^{-\alpha_J}$, with $\alpha_J \leq 1$ [64]. In one dimension, the random antiferromagnetic short range Heisenberg model is known to flow at low temperature to the infinite randomness fixed point, where the ground state is formed of randomly placed spin singlets [107]. When the localization length ξ exceeds the Fermi wave length, however, the indirect exchange interaction oscillates in sign with distance, as the RKKY interaction in the metallic regime, but decays exponentially beyond ξ . In the next section we will address the question, whether the RKKY interaction or the Kondo effect wins the spin competition in disordered electron systems in the vicinity of the delocalization transition.

7.4 Doniach diagram of disordered systems

Extending the argument of Doniach [13] to disordered systems where both Kondo temperature T_K and RKKY couplings are distributed, it is natural to study next the distribution of the ratio of both energy scales, $J_{\text{RKKY}}(\mathbf{r}_{ij})$ and T_{K_i} . This has been done in Ref. [88], as shown in Fig. 14(left) for four distances R between two magnetic moments, placed randomly in a 2D disordered tight binding model. While it is found to have a wide distribution for all R , there

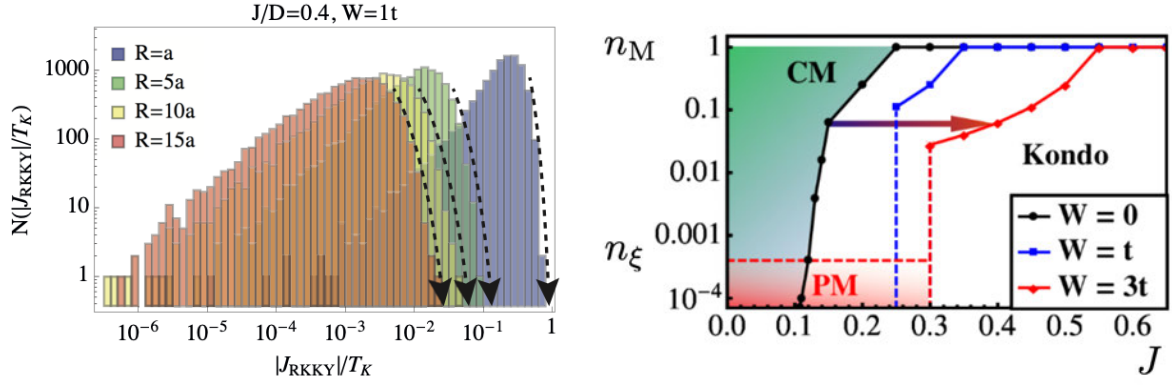


Fig. 14: *Left: Distribution of ratio $|J_{\text{RKKY}}(R)|/T_K$ for two magnetic moments at distance R , placed randomly in a 2D disordered lattice. Black arrows: sharp cutoff. Right: Magnetic quantum phase diagram, critical density of magnetic moments n_c as function of J for various disorder strengths W , as derived numerically from that cutoff, separating a coupled moment (CM) from a Kondo screened phase. Horizontal dashed line separates the free moment phase (PM) for $J < J_c(W)$, and $n_M < n_\xi$, where n_ξ is the concentration, when there is no more than one magnetic moment within a localization length ξ . Linear system size $L = 100a$, number of disorder configurations $M = 30000$. Figs. taken from Ref. [88].*

is a sharp cutoff, indicated by the black arrows. From the condition that $|J_{\text{RKKY}}(R)/T_K| < 1$ for all concentrations $n_M = 1/R^d$ below a critical value $n_c = 1/R_c^d$, we can derive n_c accurately as function of exchange coupling J . The resulting quantum phase diagram is shown in Fig. 14(right) for three disorder strengths W . The Kondo dominated regime is pushed to larger J as the disorder strength W is increased. At strong disorder a phase of uncoupled, paramagnetic local moments (PM) appears at small $n_M < n_\xi$, where n_ξ is the concentration, when there is no more than one magnetic moment within the range of a localization length ξ , as shown in Fig. 14(right) (horizontal red dashed line) [88].

In Fig. 15 we show the critical coupling $J_c^{(1)}$ as function of disorder amplitude W , as defined to be the coupling above which there remain no unscreened magnetic moments in the sample. It is derived for a 2D disordered tight binding model as function of disorder amplitude W with (left figure) numerical exact diagonalization for several lengths L . The full line is a plot of $J_c^A(W)$, Eq. (49), with 2D localization length $\xi = l_e \exp(\pi E_F \tau)$, where $1/\tau = \pi W^2/(6D)$. The dashed line is a guide to the eye. In Fig. 15(right) we show results obtained by employing the Kernel polynomial method for Eq. (9) for system size $L = 100$ [88]. The dashed line is the analytical function $J_c^{(1)}(W)$, obtained from deriving the density of free moments due to local pseudo-gaps, yielding $J_c^{(1)} = \sqrt{\eta}D/2$, with $\eta = 2(\alpha_0 - d)/d$. In $d = 2$, expansion in $1/g$, with $g = E_F \tau$, yields $\eta = 2/(\pi g)$ and thus

$$J_c^{(1)}(W) = \sqrt{\frac{D}{3E_F}} W. \quad (57)$$

The good agreement with numerical results supports the result that the formation of free moments is due to local pseudo-gaps formed by multifractal intensity distribution and correlations. To go beyond the Doniach argument for disordered systems let us next apply and extend the self

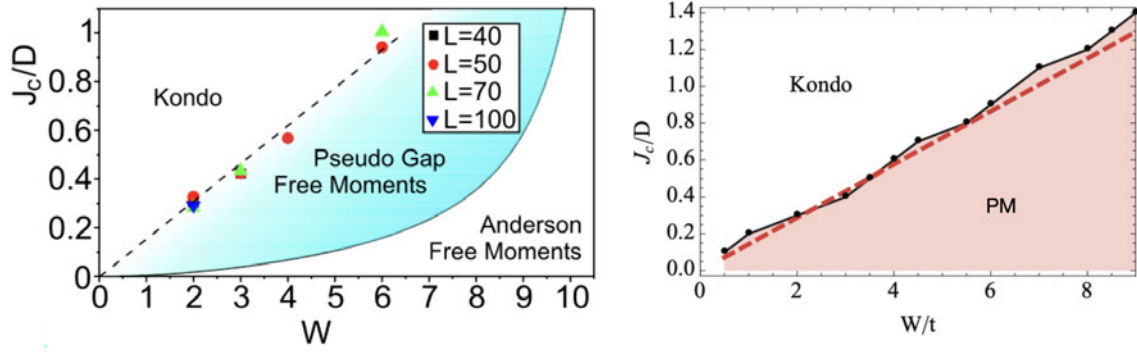


Fig. 15: *Left: Critical coupling $J_c^{(1)}$ as function of disorder amplitude W , derived for a 2D disordered tight binding model as function of disorder amplitude W with numerical exact diagonalization for sizes L , defined such that for $J > J_c^{(1)}$, there is no unscreened magnetic moment in the sample. Full line: $J_c^A(W)$, Eq. (49), with 2D localization length $\xi = l_e \exp(\pi E_F \tau)$, where $1/\tau = \pi W^2/(6D)$. Dashed line: guide to the eye. Fig. taken from Ref. [102]. Right: Same as left figure, but derived by employing Kernel polynomial method to Eq. (9) for $L = 100$ [88]. Dashed line: analytical function $J_c^{(1)}(W)$, Eq. (57). Fig. taken from Ref. [88].*

consistent approach of Ref. [54], reviewed in section 5. Placing two magnetic moments at sites of a disordered electron system with different local density of states yields different bare Kondo temperatures $T_{K_i}^0 = D_0 \exp(-1/(2g_i^0))$, $i = 1, 2$ [58]. By solving the coupled RG-Eqs. (29) for two magnetic moments numerically, we find that both Kondo temperatures are reduced in the presence of RKKY-coupling, see Fig. 16. The initially smaller Kondo temperature T_{K_2} is suppressed more than the larger one T_{K_1} . Thereby, their ratio $x = T_{K_2}/T_{K_1}$ decreases. Thus, we find that the inequality between Kondo temperatures becomes enhanced by RKKY coupling. Moreover, the quenching of the Kondo screening by the RKKY coupling occurs already for smaller RKKY coupling, as seen in Fig. 16(left), the stronger the inhomogeneity and the smaller the ratio of the bare Kondo temperature x_0 . For the smallest value, $x_0 = 0.1$, the breakdown occurs at a critical value $y_c(x_0 \ll 1) = 0.88y_c$, where y_c is the one in the homogeneous system, Eq. (35). The discontinuous jump of both Kondo temperatures T_{K_1} and T_{K_2} at $y_c(x_0)$ are seen in Fig. 16(right), plotted relative to their bare values as function of bare Kondo temperature ratio x_0 and dimensionless RKKY coupling parameter \tilde{y} . Thus, we conclude that disorder makes Kondo screening more easily quenched by RKKY coupling.

For a finite density of randomly distributed magnetic moments n_M , coupled by random local exchange couplings J_i^0 to conduction electrons with random local density of states $\rho(E, \mathbf{r}_i)$, one can extend this approach, solving the coupled RG-Eqs. (29). Every magnetic moment has then, in general, a different Kondo temperature, as they are placed at different positions with different local couplings $g_0(\mathbf{r}_i) = J_i^0 \rho(E, \mathbf{r}_i)$. As the RKKY coupling is itself distributed widely in disordered systems [85, 88] the long range function $y(\mathbf{r}-\mathbf{r}')$ is distributed as well. We can thus derive the distribution function of Kondo temperatures T_K from Eqs. (29). We note that the random distribution of RKKY-couplings is mainly due to the distribution of local couplings $g_0(\mathbf{r})$ [88], while the function $y(\mathbf{r}-\mathbf{r}')$ is only weakly affected by the disorder.

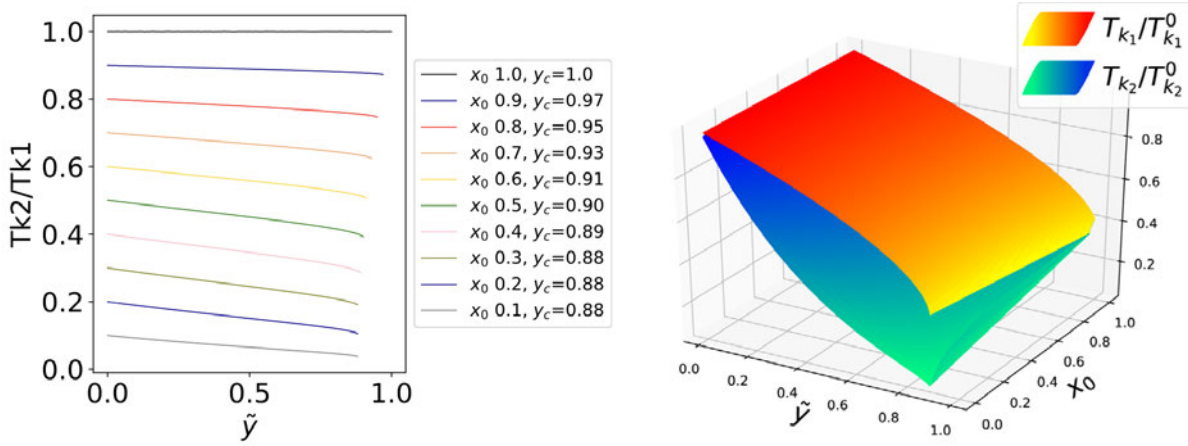


Fig. 16: *Left: The ratio of Kondo temperatures of two magnetic moments $x = T_{K2}/T_{K1}$ as function of dimensionless RKKY coupling parameter \tilde{y} , relative to its critical value y_c for the homogenous system, for different bare Kondo temperature ratios $x_0 = T_{K2}^0/T_{K1}^0$. It stops at a critical value $\tilde{y}_c(x_0)$, relative to y_c for the homogenous system. Right: Kondo temperatures T_{K1} and T_{K2} relative to their bare values as function of bare Kondo temperature ratios x_0 and the dimensionless RKKY coupling parameters \tilde{y} . Figs. are taken from Ref. [58].*

Without the RKKY-coupling we found at the mobility edge a bimodal distribution of T_K with one peak close to the Kondo temperature of the clean system and a power law divergent tail at low T_K [88, 103, 104], see Fig. 13. Since the RKKY-interaction enhances inequalities between Kondo temperatures, we expect that it shifts more weight to the low Kondo temperature tail. This could be checked quantitatively by the solution of Eqs. (29), but still needs to be done.

Anderson localization is weakened when time reversal and spin symmetry are broken by magnetic scattering from magnetic moments [108, 109]. A finite magnetic scattering rate τ_s^{-1} enhances the localization length through the parameter $X_s = \xi^2/L_s^2$, where $L_s = \sqrt{D_e\tau_s}$ is the spin relaxation length [110] and $D_e = v_F^2\tau/3$ the electron diffusion coefficient. When $X_s \geq 1$ the electron spin relaxes before it covers the area limited by ξ , and Anderson localization is weakened. In 3D the mobility edge is thereby shifted towards stronger disorder by magnetic scattering. As Kondo screening of magnetic moments diminishes magnetic scattering, while RKKY coupling tries to quench their spins, resulting in magnetic scattering, the competition between these effects governs Anderson localization and the position of the delocalization transition. Treating the interplay between Anderson localization and Kondo screening, novel effects like a giant magneto resistance [106, 103], finite temperature delocalization transitions and the emergence of a critical band [103] have been derived. Experimentally, the interplay of Kondo effect, indirect exchange interaction and Anderson localization has recently been studied in a 2D experimental setup in a controlled way [111]. Thus, it remains an important and experimentally relevant problem, to develop a self consistent treatment of Anderson localization, Kondo screening and RKKY-coupling. This problem has been studied with the disordered Kondo lattice and the Anderson-Hubbard model with a variety of numerical methods. Each method comes with different approximations, providing different insights. These include mean-field theories of the Kondo lattice with an added RKKY coupling term [44, 112–117], where fluctuations around the mean-field theory have been studied with Ginzburg-Landau and nonlinear sigma model type

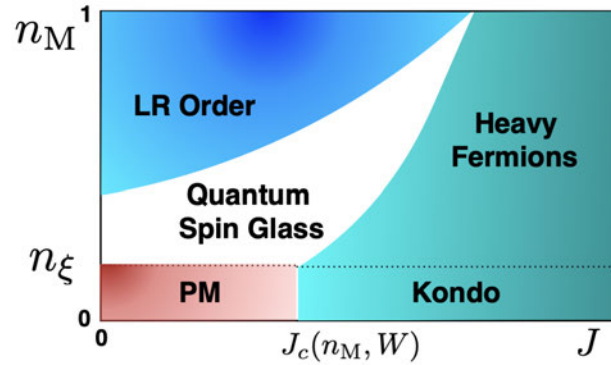


Fig. 17: Schematic quantum phase diagram of Kondo lattice systems as function of magnetic moment density n_M and exchange coupling J for fixed disorder W . The critical coupling $J_c(n_M, W)$ separates spin coupled from Kondo screened phases. Dark blue indicates higher transition temperatures to the long range ordered state (LR). Dark red indicates higher concentrations of free magnetic moments (PM), when electrons are localized and there is not more than one magnetic moment within the localization length ξ , $n_M < n_\xi = \xi^{-d}$. Dark petrol indicates higher Kondo and coherence temperatures in the dilute Kondo phase and heavy fermion phase.

actions. Statistical dynamical mean-field theory based approaches [118–125], Hartree-Fock based methods [126–128], quantum Monte Carlo method [129–132], typical medium dynamics cluster approximations [133, 134] and cluster extensions of the numerical renormalization group method [135] have been applied. While we cannot review all results, some of them have been reviewed in Ref. [90], we would like to mention that in Refs. [133, 134] the quasiparticle self energy of the Anderson-Hubbard model was derived as function of excitation energy $\text{Im} \Sigma(\omega) \sim \omega^{\alpha_\Sigma}$. It was found to behave as a non-Fermi liquid with power $\alpha_\Sigma(W) < 2$, which becomes smaller with stronger disorder amplitude W . The non-Fermi liquid phase extends down to lowest energies at the mobility edge. Away from it, it is cutoff by $\Delta_\xi = 1/(\rho\xi^d)$, and $\Delta_{\xi_c} = 1/(\rho\xi_c^d)$, respectively. This is in agreement with the phase diagram derived from the magnetic properties, reviewed above, Fig. 13(right). The typical medium dynamics cluster approximation employed in Ref. [133] does not include long range indirect exchange interactions. Thus, the study of the competition between Anderson localization, Kondo screening and RKKY-coupling, remains a challenging problem.

8 Conclusions and open problems

To conclude, when magnetic moments are immersed into the Fermi sea of itinerant electrons, rich quantum physics emerges, which is relevant for a wide range of materials including heavy Fermion systems, materials with $4f$ or $5f$ atoms, notably Ce, Yb, or U, high temperature superconductors like the cuprates, but also good metals with magnetic impurities, doped semiconductors like Si:P close to the metal-insulator transition, 2D materials like graphene and topological insulators. While each material has its specific properties, requiring detailed modelling, their electronic properties are to some degree governed by the competition between Kondo screening and indirect exchange couplings, which can be modelled by (disordered) Kondo lattices. We summarize the main results in the schematic quantum phase diagram Fig. 17.

While the Doniach argument gives a good idea of the competition between Kondo screening and RKKY coupling, a self consistent renormalization theory which implements the RKKY coupling into the Kondo renormalization yields a remarkably different result: the Kondo temperature jumps discontinuously to zero at a critical exchange coupling which is larger than expected with the Doniach argument. We reviewed the extension of that framework to a finite density of magnetic moments n_M to systems with a spectral (pseudo) gap and to disordered systems, where the Kondo temperature is different for every magnetic moment. We have seen that disorder leads to a wide distribution of both Kondo temperature and RKKY couplings and tends to diminish the Kondo dominated phase, enhancing the critical coupling $J_c(n_M, W)$. In the dilute limit we identified a paramagnetic phase, even at zero temperature, where the Kondo screening is prevented by local pseudo-gaps, and the RKKY coupling between the dilute magnetic moments is cutoff by Anderson localization. In that regime, the density of free magnetic moments is found to decrease continuously with increasing J . There, an analytical formula for the increase of the critical coupling $J_c^{(1)}(n_M, W)$ with disorder W is available, Eq. (57), which was found in 2D to be in good agreement with numerical results, see Fig. 15.

As the density of magnetic moments is increased, there is a succession of quantum phase transitions between quantum spin glass and ordered phases for couplings $J < J_c(n_M, W)$, as shown schematically in Fig. 17. Since we cannot review here the rich physics and variety of these spin coupled phases, let us refer to the literature cited above and recent reviews [8, 90, 44, 65]. For $J > J_c(n, W)$, a transition between a phase of dilute Kondo singlets and a heavy fermion state is expected as n_M is increased. Experimentally, even for dilute densities of about $n_M = 0.05$, indications of a coherent Kondo lattice were found in Si:P deep in the metallic phase [136] and in the dilute Kondo lattice CeIn₃ [137]. The theory of the transition from dilute Kondo singlets to heavy Fermions is still a challenging problem, as it requires to solve the dilute Kondo lattice model, as studied for example in [132]. Taking fully into account the disorder introduced by the random placements of magnetic moments is still a challenge. Last but not least, even in the dense magnetic moment limit $n_M \rightarrow 1$, the mechanism for the emergence of long range order at the Kondo breakdown is under debate. Is it due to the ordering of emerging local moments, or a spin-density wave transition [8] or a more complex mechanism, where ordered magnetic moments and Kondo screening coexist in a spatially modulated state [138]?

Acknowledgements

These lecture notes are dedicated to the memory of Peter Fulde. We thank Hans Kroha and Keith Slevin for critical reading and feedback

References

- [1] J. Kondo, *Prog. Theor. Phys* **32**, 37 (1964)
- [2] A.C. Hewson: *The Kondo Problem to Heavy Fermions* (Cambridge Univ. Press, 1993)
- [3] P. Mohanty and R.A. Webb, *Phys. Rev. Lett.* **84**, 4481 (2000); *ibid.* **91**, 066604 (2003)
- [4] F. Pierre and N.O. Birge, *Phys. Rev. Lett.* **89**, 206804 (2002)
- [5] F. Mallet, J. Ericsson, D. Mailly, S. Ünlübayir, D. Reuter, A. Melnikov, A.D. Wieck, T. Micklitz, A. Rosch, T.A. Costi, L. Saminadayar, and C. Bäuerle, *Phys. Rev. Lett.* **97**, 226804 (2006)
- [6] P. Nozières, *J. Low Temp. Phys.* **17**, 3 (1974)
- [7] P. Nozières, *Eur. Phys. J. B* **6**, 447 (1998)
- [8] P. Coleman: *Heavy Fermions: electrons at the edge of magnetism*, in H. Kronmüller and S. Parkin (eds.): *Handbook of Magnetism and Advanced Magnetic Materials, Vol 1: Fundamentals and Theory* (Wiley, New York, 95-148, 2007)
- [9] P. Fulde: *Correlated Electrons in Quantum Matter* (World Scientific, Singapore, 2012)
- [10] M.A. Ruderman and C. Kittel, *Phys. Rev.* **96**, 99 (1954)
- [11] T. Kasuya, *Prog. Theor. Phys.* **16**, 45 (1956)
- [12] K. Yosida, *Phys. Rev.* **106**, 893 (1957)
- [13] S. Doniach, *Physica B+C* **91** 231(1977)
- [14] J. Kroha: *Interplay of Kondo effect and RKKY interaction*, in E. Pavarini, Erik Koch, R. Scalettar, and R.M. Martin (eds.): *The Physics of Correlated Insulators, Metals, and Superconductors Modeling and Simulation, Vol. 7* (Forschungszentrum Jülich, 2017)
- [15] P.W. Anderson, *Phys. Rev.* **124**, 41 (1961)
- [16] J.R. Schrieffer and P. Wolff, *Phys. Rev.* **149**, 491 (1966)
- [17] Y. Nagaoka, *Phys. Rev.* **138**, 1112 (1965)
- [18] H. Suhl, *Phys. Rev. A* **138**, 515 (1965)
- [19] P.W. Anderson, G. Yuval, and D.R. Hamann, *Phys. Rev. B* **1**, 4464 (1970)
- [20] G. Zarand and L. Udvardi, *Phys. Rev. B* **54**, 7606 (1996)
- [21] K. G. Wilson, *Rev. Mod. Phys.* **47**, 773 (1975)
- [22] H.R. Krishna-murthy, J.W. Wilkins, and K.G. Wilson, *Phys. Rev. B* **21**, 1003 (1980); *ibid.* **21**, 1044 (1980)

- [23] A.M. Tsvelick and P.B. Wiegmann, *Adv. Phys.* **32**, 453 (1983)
- [24] N. Andrei, K. Furuya, and J.H. Lowenstein, *Rev. Mod. Phys.* **55**, 331 (1983)
- [25] P. Nozières, *J. Phys. C*, **37**, 1 (1976)
- [26] S. Kettemann, E.R. Mucciolo, *JETP Lett.* **83**, 240 (2006)
- [27] T. Micklitz, A. Altland, T.A. Costi, and A. Rosch, *Phys. Rev. Lett.* **96**, 226601 (2006)
- [28] S. Kettemann and E.R. Mucciolo, *Phys. Rev. B* **75**, 184407 (2007)
- [29] A.A. Abrikosov, L.L.P. Gorkov, I.E. Dzialosinskij, and I.I.E. Dzialoshinskii: *Methods of Quantum Field Theory in Statistical Physics* (Dover Publications, 1975)
- [30] D.N. Aristov, *Phys. Rev. B* **55**, 8064 (1997)
- [31] F. Meier, L. Zhou, J. Wiebe and R. Wiesendanger, *Science* **320**, 82 (2008)
- [32] S. Seiro, L. Jiao, S. Kirchner *et al.*, *Nat Commun.* **9**, 3324 (2018)
- [33] A. Menth, E. Buehler, and T.H. Geballe, *Phys. Rev. Lett.* **22**, 295 (1969)
- [34] B. Coqblin and J.R. Schrieffer, *Phys. Rev.* **185**, 847 (1969)
- [35] N. Read and D.M. Newns, *J. Phys. C* **16**, L1055 (1983); *ibid.* **16**, 3273 (1983)
- [36] A. Auerbach and K. Levin, *Phys. Rev. Lett.* **57**, 877 (1986)
- [37] W. Metzner, and D. Vollhardt, *Phys. Rev. Lett.* **62**, 324 (1989)
- [38] M. Jarrell, *Phys. Rev. B*, **51**, 7429 (1995)
- [39] A. Georges, G. Kotliar, W. Krauth, and M. Rozenberg, *Rev. Mod. Phys.* **68**, 13 (1996)
- [40] H. Schweitzer and G. Czycholl, *Phys. Rev. Lett.* **67**, 3724 (1991)
- [41] A.Theumann, B. Coqblin, S.G. Magalhaes and A.A. Schmidt, *Phys. Rev. B* **63**, 054409 (2001)
- [42] B. Coqblin, J.R. Iglesias, N.B. Perkins, S.G. Magalhaes and F.M. Zimmer, *J. Magn. Magn. Mater.* **320**, 1989 (2008)
- [43] S.G. Magalhaes, F.M. Zimmer, and B. Coqblin, *Phys. Rev. B* **81**, 094424 (2010)
- [44] S.G. Magalhaes, F. Zimmer and B. Coqblin, *Int. J. Mod. Phys. Conf. Ser.* **11**, 38 (2012)
- [45] B.A. Jones and C.M. Varma, *Phys. Rev. Lett.* **58**, 843 (1987)
- [46] R. Bulla, T.A. Costi, and T. Pruschke, *Rev. Mod. Phys.* **80**, 395 (2008)
- [47] F. Eickhoff, B. Lechtenberg, and F.B. Anders, *Phys. Rev. B* **98**, 115103 (2018)
- [48] A.K. Mitchell and R. Bulla, *Phys. Rev. B* **92**, 155101 (2015)

- [49] F. Eickhoff and F.B. Anders, Phys. Rev. **B 102**, 205132 (2020)
- [50] J. Bork, Y.-H. Zhang, L. Diekhöner, L. Borda, P. Simon, J. Kroha, P. Wahl, and K. Kern, Nat. Phys. **7**, 901 (2011)
- [51] A. Gleis, S.-S.B. Lee, G. Kotliar, and J. von Delft, arXiv:2310.12672 (2023)
- [52] S. Fujimoto and N. Kawakami, J. Phys. Soc. Jpn. **66**, 2157 (1997)
- [53] H. Tsunetsugu, M. Sigrist, and K. Ueda, Rev. Mod. Phys. **69**, 809 (1997)
- [54] A. Nejati, K. Ballmann, and J. Kroha, Phys. Rev. Lett. **118**, 117204 (2017)
- [55] K. Matho and M.T. Béal-Monod, Phys. Rev. **B 5**, 1899 (1972); *ibid.* **B 6**, 2888 (1972)
- [56] Y.C. Tsay and M.W. Klein, Phys. Rev. **B 7**, 352 (1973)
- [57] Y.C. Tsay and M.W. Klein, Phys. Rev. **B 11**, 318 (1975)
- [58] K.-Y. Park, I. Jang, K.-S. Kim and S. Kettemann, Ann. Phys. **435**, 168501 (2021)
- [59] D. Withoff and E. Fradkin, Phys. Rev. Lett. **64**, 1835 (1990); K. Ingersent, Phys. Rev. B **54**, 11936 (1996); S. Florens and M. Vojtá, Phys. Rev. B **72**, 115117 (2005); L. Fritz, S. Florens, and M. Vojtá, Phys. Rev. B **74**, 144410 (2006)
- [60] D. Sherrington and S. Kirkpatrick, Phys. Rev. Lett. **35**, 1792 (1975)
- [61] G. Forestier, M. Solana, C. Naud, A.D. Wieck, F. Lefloch, R. Whitney, D. Carpentier, L.P. Lévy and L. Saminadayar, Phys. Rev. **B 102**, 024206 (2020)
- [62] J.C. Gomez Sal, J. Garcia Soldevilla, J.A. Blanco, J.I. Espeso, J. Rodriguez Fernandez, F. Luis, F. Bartolome, Phys. Rev. B **56**, 11741 (1997)
- [63] T. Westerkamp, M. Deppe, R. Kuchler, M. Brando, C. Geibel, P. Gegenwart, A.P. Pikul and F. Steglich, Phys. Rev. Lett. **102**, 206404 (2009)
- [64] R.N. Bhatt, P.A. Lee, Phys. Rev. Lett. **48**, 344 (1982)
- [65] S. Kettemann, Special Issue in memory of K.B. Efetov, Ann. Phys. **456**, 169306 (2023)
- [66] K. Sato, L. Bergqvist, J. Kudrnovský, P.H. Dederichs, O. Eriksson, I. Turek, B. Sanyal, G. Bouzerar, H. Katayama-Yoshida, V.A. Dinh, T. Fukushima, H. Kizaki, and R. Zeller, Rev. of Mod. Phys. **82**, 1633 (2010)
- [67] M.Z. Hasan and C.L. Kane Rev. Mod. Phys. **82**, 3045 (2010)
- [68] A.H. Castro Neto, F. Guinea, N.M.R. Peres, K.S. Novoselov, and A.K. Geim, Rev. Mod. Phys. **81**, 109 (2009)
- [69] M.T. Glossop and K. Ingersent, Phys. Rev. B. **75** 104410 (2007)
- [70] M. Vojtá and R. Bulla, Eur. Phys. J. B **28**, 283 (2002)

- [71] S. Saremi and P.A. Lee, Phys. Rev. **75**, 165110 (2007)
- [72] H.Y. Lee and S. Kettemann, Phys. Rev. B **91**, 205109 (2015)
- [73] M. Sherafati and S. Satpathy, Phys. Rev. **B 83**, 165425 (2011)
- [74] P.W. Anderson, Nobel Lectures in Physics **1980**, 376 (1977)
- [75] N.F. Mott, J. Phys. Colloques **37**, C4 (1976)
- [76] E. Miranda, V. Dobrosavljevic, and G. Kotliar, J. Phys.: Condens. Matter **8**, 9871 (1996)
- [77] R.N. Bhatt and D.S. Fisher, Phys. Rev. Lett. **68**, 3072 (1992)
- [78] A. Langenfeld and P. Woelfle, Ann. Phys. **507**, 43 (1995)
- [79] P.S. Cornaglia, D.R. Grempel, and C.A. Balseiro, Phys. Rev. Lett. **96**, 117209 (2006)
- [80] A.D. Mirlin, Phys. Rep. **326**, 259 (2000)
- [81] P.G. de Gennes, J. Phys. Radium **23**, 630 (1962)
- [82] A.Y. Zyuzin and B.Z. Spivak, JETP Lett. **43** 234 (1986)
- [83] L.N. Bulaevskii and S.V. Panyukov, JETP Lett. **43**, 240 (1986)
- [84] G. Bergmann, Phys. Rev. **B 36**, 2469 (1987)
- [85] I.V. Lerner, Phys. Rev. **B 48**, 9462 (1993)
- [86] H.Y. Lee, E.R. Mucciolo, G. Bouzerar, S. Kettemann, Phys. Rev. **B 86**, 205427 (2012)
- [87] H.Y. Lee, J.H. Kim, E.R. Mucciolo, G. Bouzerar, and S. Kettemann, Phys. Rev. **B 85**, 075420 (2012)
- [88] H.Y. Lee and S. Kettemann, Phys. Rev. **B 89**, 165109 (2014)
- [89] H. von Löhneysen, Ann. Phys. (Berlin) **523**, 599 (2011)
- [90] E. Miranda and V. Dobrosavljevic, Rep. Prog. Phys. **68**, 2337 (2005)
- [91] P. A. Lee and T.V. Ramakrishnan, Rev. Mod. Phys. **57**, 287 (1985)
- [92] B. Kramer and A. MacKinnon, Rep. Prog. Phys. **56**, 1469 (1993)
- [93] D. Belitz and T. Kirkpatrick, Rev. Mod. Phys. **66** (1994)
- [94] K.B. Efetov: *Supersymmetry in Disorder and Chaos*, (Cambridge Univ. Press, 1997)
- [95] B. Kramer, T. Ohtsuki, and S. Kettemann, Phys. Rep. **417**, 211 (2005)
- [96] F. Evers and A. Mirlin, Rev. Mod. Phys. **80**, 63 (2008)
- [97] R.N. Bhatt and S. Kettemann, Special Issue Localization 2020: Editorial Summary, Ann. Phys. **435**, 168664 (2021)

- [98] A. Richardella, P. Roushan, S. Mack, B. Zhou, D.A. Huse, D.D. Awschalom, A. Yazdani, *Science* **327**, 665 (2010)
- [99] J. Gao, J.W. Park, K.-S. Kim, S.K. Song, H.R. Park, J. Lee, J. Park, F. Chen, X. Luo, Y. Sun, and H.W. Yeom, *Nano Lett.* **20**, 6299 (2020)
- [100] J.T. Chalker, *Physica A* **167**, 253 (1990); V.E. Kravtsov and K.A. Muttalib, *Phys. Rev. Lett.* **79**, 1913 (1997); J.T. Chalker *et al.*, *JETP Lett.* **64**, 386 (1996); T. Brandes, B. Huckestein, and L. Schweitzer, *Ann. Phys. (Leipzig)* **5**, 633 (1996)
- [101] E. Cuevas and V.E. Kravtsov, *Phys. Rev. B* **76**, 235119 (2007)
- [102] A. Zhuravlev, I. Zharekeshev, E. Gorelov, A.I. Lichtenstein, E.R. Mucciolo, and S. Kettemann, *Phys. Rev. Lett.* **99**, 247202 (2007)
- [103] S. Kettemann, E.R. Mucciolo, I. Varga, and K. Slevin, *Phys. Rev. B* **85**, 115112 (2012)
- [104] K. Slevin, S. Kettemann, and T. Ohtsuki, *Eur. Phys. J. B* **92**, 281(2019)
- [105] M. Debertolis, I. Snyman, and S. Florens, *Phys. Rev. B* **106** 125115 (2022)
- [106] S. Kettemann and M.E. Raikh, *Phys. Rev. Lett.* **90**, 146601 (2003)
- [107] F. Igloi and C. Monthus, *Phys. Rep.* **412**, 277 (2005)
- [108] D. Khmel'nitskii and A. Larkin, *Solid State Commun.* **39**, 1069 (1981)
- [109] F.J. Wegner, *Nucl. Phys. B* **270**, 1 (1986)
- [110] S. Hikami, A. Larkin, and Y. Nagaoka, *Prog. Theor. Phys.* **63**, 707 (1980)
- [111] W. Zhang, E.R. Brown, and R.P. Mirin, *Phys. Rev. Res.* **4**, 043040 (2022)
- [112] A.H. Castro Neto, G. Castilla and B.A. Jones, *Phys. Rev. Lett.* **81**, 3531 (1998); A.H. Castro Neto and B.A. Jones, *Phys. Rev. B* **62**, 14975 (2000)
- [113] M.N. Kiselev, K. Kikoin, and R. Oppermann, *Phys. Rev. B* **65**, 184410 (2002)
- [114] S. Burdin and P. Fulde, *Phys. Rev. B* **76**, 104425 (2007)
- [115] M.-T. Tran and K.-S. Kim, *Phys. Rev. Lett.* **105**, 116403 (2010)
- [116] M.-T. Tran and K.-S. Kim, *J. Phys.: Condens. Matter* **23** 425602 (2011)
- [117] B. Poudel, G. Zwicknagl, C. Lacroix, and S. Burdin, *J. of Magn. Magn. Mater.* **520**, 167405 (2021)
- [118] K. Byczuk, W. Hofstetter, U. Yu, and D. Vollhardt, *Eur. Phys. J. Spec. Top.* **180**, 135 (2009)
- [119] M. Ulmke, V. Janis, and D. Vollhardt, *Phys. Rev. B* **51**, 10411 (1995)

- [120] M.C.O. Aguiar, V. Dobrosavljevic, E. Abrahams, and G. Kotliar, Phys. Rev. **B 73**, 115117 (2006)
- [121] M.C.O. Aguiar, V. Dobrosavljevic, E. Abrahams, and G. Kotliar, Phys. Rev. Lett. **102**, 156402 (2009)
- [122] D. Tanaskovic, V. Dobrosavljevic, E. Abrahams, and G. Kotliar, Phys. Rev. Lett. **91**, 066603 (2003)
- [123] M.C.O. Aguiar and V. Dobrosavljevic, Phys. Rev. Lett. **110**, 066401 (2013)
- [124] K. Byczuk, W. Hofstetter, and D. Vollhardt, Phys. Rev. Lett. **94**, 056404 (2005)
- [125] A. Weh, Y. Zhang, A. Östlin, H. Terletska, D. Bauernfeind, K.-M. Tam, H.G. Evertz, K. Byczuk, D. Vollhardt, and L. Chioncel, Phys. Rev. **B 104**, 045127 (2021)
- [126] M. Milovanović, S. Sachdev, and R. N. Bhatt, Phys. Rev. Lett. **63**, 82 (1989)
- [127] S. Sachdev, Phil. Trans. R. Soc. **A 356**, 173 (1998)
- [128] M.A. Tusch and D.E. Logan, Phys. Rev. **B 48**, 14843 (1993)
- [129] P.B. Chakraborty, K. Byczuk, and D. Vollhardt, Phys. Rev. **B 84**, 035121 (2011)
- [130] M. Ulmke and R.T. Scalettar, Phys. Rev. **B 55**, 4149 (1997)
- [131] M.E. Pezzoli and F. Becca, Phys. Rev. **B 81**, 075106 (2010)
- [132] N.C. Costa, T. Mendes-Santos, T. Paiva, N.J. Curro, R.R. dos Santos, and R.T. Scalettar, Phys. Rev. **B 99**, 195116 (2019)
- [133] S. Sen, N.S. Vidhyadhiraja, M. Jarrell, Phys. Rev. **B 98**, 075112 (2018)
- [134] C.E. Ekuma, H. Terletska, K.-M. Tam, Z.-Y. Meng, J. Moreno, and M. Jarrell, Phys. Rev. **B 89**, 081107 (2014)
- [135] A.K. Mitchell, P.G. Derry, and D.E. Logan, Phys. Rev. **B 91**, 235127 (2015)
- [136] H. Im, D.U. Lee, J. Jo, Y. Chong, W. Song, H. Kim, E.K. Kim, T. Yuk, S.-J. Sin, S. Moon, J.R. Prance, Y.A. Pashkin, J.S. Tsai, Nat. Phys. **19**, 676 (2023)
- [137] C.-K. Park, S. Park, H. Jang, T.B. Park, I.C. Kim, S. Shin, T. Lee, T. Fennell, U. Stuhr, M. Kenzelmann, H. Lee, and T. Park, J. Korean Phys. Soc. **84**, 446 (2024)
- [138] P. Li, H. Ye, Y. Hu, Y. Fang, Z. Xiao, Z. Wu, Z. Shan, R.P. Singh, G. Balakrishnan, D. Shen, Y-f. Yang, C. Cao, N.C. Plumb, M. Smidman, M. Shi, J. Kroha, H. Yuan, F. Steglich, and Y. Liu, Phys. Rev. **B 107**, L201104 (2023)